SERV_FORFIRE

Report on the Case study demonstration

M.6

Issued on 07/07/2020

Table of contents

Table of figures

1. Fire risk estimation: pre-fire phase

1.1 Demonstration of the six-week forest fire danger outlooks in Finland

Contribution by FMI: Vajda A, Wolff C., Hyvärinen O., Kolstela J.

The statistical model developed in the first phase of the project to predict the seasonal and sub-seasonal (six week) forest fire danger have been first evaluated for Finnish conditions followed by a demonstration of the sub-seasonal forest fire risk outlook prototype with users during the summer season 2019.

The model was evaluated using re-forecast data from ECMWF's extended range forecast system (EPS) and seasonal forecast system (SEAS5) (ECMWF 2016, 2018) for the time period 2008 to 2016. The predicted FFI and the input parameters were verified against observations using standard verification methodologies. The predicted potential fire risk (FFI>4.0) was underestimated by the model for both sub-seasonal and seasonal scale. On sub-seasonal scale temperature had the highest skill of the parameters, but the skill of both and RH was lower consisting of a significant drop after the first lead week (Fig. 1). Following the evaluation, model improvements have been done, e.g. including an adjustment period of one week from observations, thus the model is initialized with the current soil conditions which fosters the stabilization of the model.

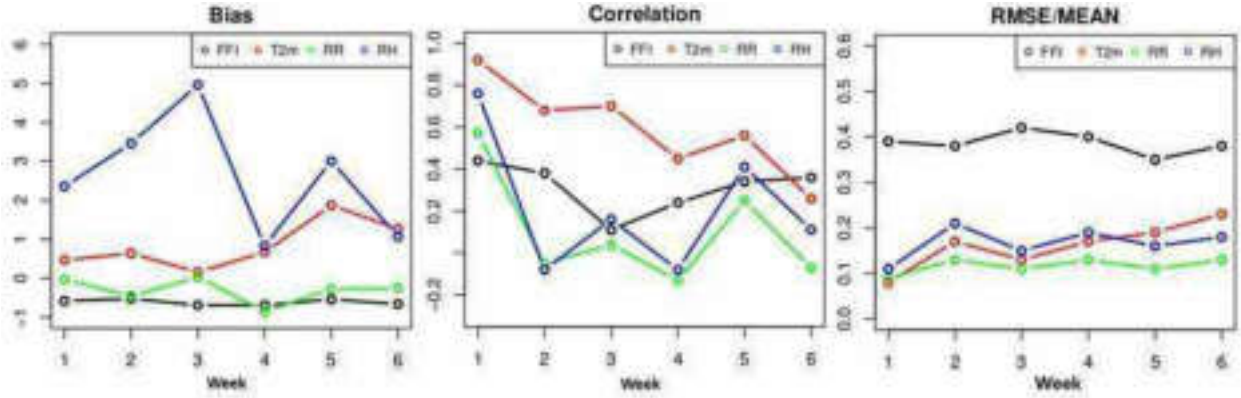

Figure 1 - Verification metrics (bias, correlation and RMSE/MEAN) for predicted FFIs and the input parameters (T, RR and RH). The weekly mean metric is calculated for various lead weeks (weeks 1 to 6) for the time period 2008-2016.

The developed statistical model was used in the production of sub-seasonal forest fire risk outlooks prototype, which is being piloted with end-users during summer season 2019. The users testing the prototype were the Regional State Administrative Agency from Northern Finland, Finnish Rescue Services - North Karelia and Department for Rescue Services from the Ministry of the Interior. The use of sub-seasonal forest fire risk outlook would allow Rescue Services to prepare in advance and plan the fire survey flights according to the expected risk.

The six-week (sub-seasonal) fire risk outlooks were produced operationally and delivered twice a week to the Rescue Services during June–September. The outlooks expressed the probability forecast of forest fire risk for Finland. For the production and dissemination of the six week outlooks the operational service set-up earlier in FMI within the SA CLIPS project for the

extended–range forecast products was utilized which implies a fully operational and automatized run. A detailed description of the operational service is given in Vajda et al. (submitted), the schematic diagram of the production flow and data processing steps using in the operational production and dissemination of the outlooks are presented in Figure 2.

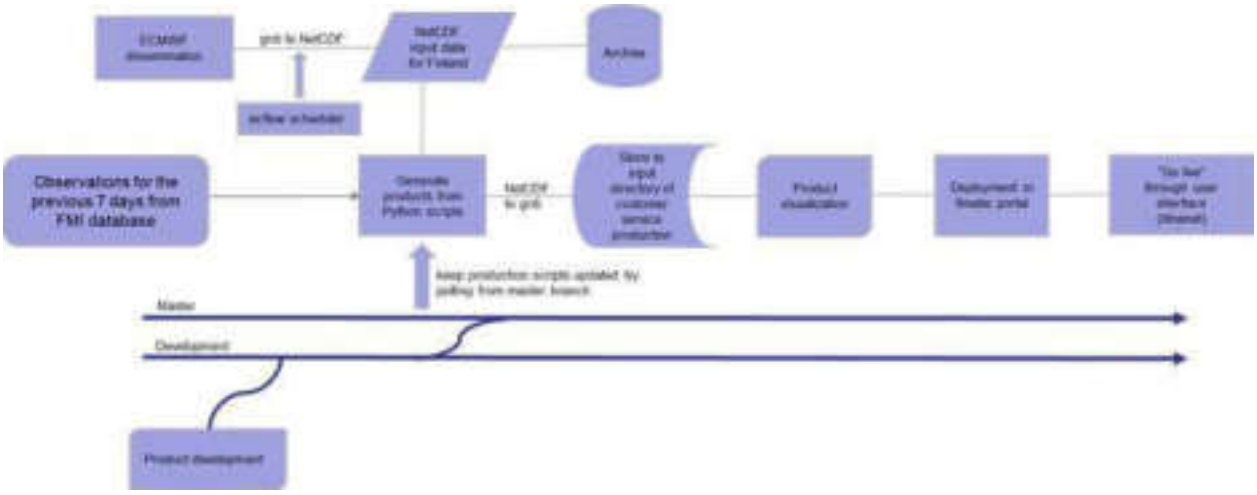

Figure 2 - The schematic diagram of the production flow and data processing steps used in the operational service of the six week fire risk outlooks (modified from Vajda et al. submitted).

The "real-time" forecast of 2 m temperature, total precipitation and relative humidity were extracted from ECMWF EPS system. The retrieval of parameters was automatized using the dissemination stream from FMI's operational system. A typical production run begun after a new forecast has been disseminated to FMI, i.e., every Monday and Thursday. The climate outlooks were communicated with the pilot users through an online user interface implemented by the research team. Once the updates of the climate outlook were brought into production, the produced weekly maps were exported first to an internal management tool (Ilmatie) where the product and its content was organized and the finalized sub-seasonal fire risk outlooks were displayed on the user interface, i.e., the Ilmanet service platform, which end-users have had access to. The climate outlooks displayed included six static weekly maps presenting the predicted forest fire risk conditions for Finland during the forecast week expressed as probability and an animated runs of the weekly maps showing fire weather conditions during the weeks 1-6 (Fig. 3). Daily probabilities were defined as the percentage of forecast ensemble members indicating a fire risk, i.e. FFI≥4. Weekly probabilities were defined as the weekly mean of daily probabilities. Finally, these probabilities were expressed as probability categories between 5% and 95%. The updated climate outlooks were available for the users every Tuesday and Friday. The first climate outlooks were released in June and the run continues until the end of fire season (September).

Following the release of the first six week forest fire risk outlook informational material was provided and a guiding session was organized for the users in order to facilitate the use and interpretation of forecasts.

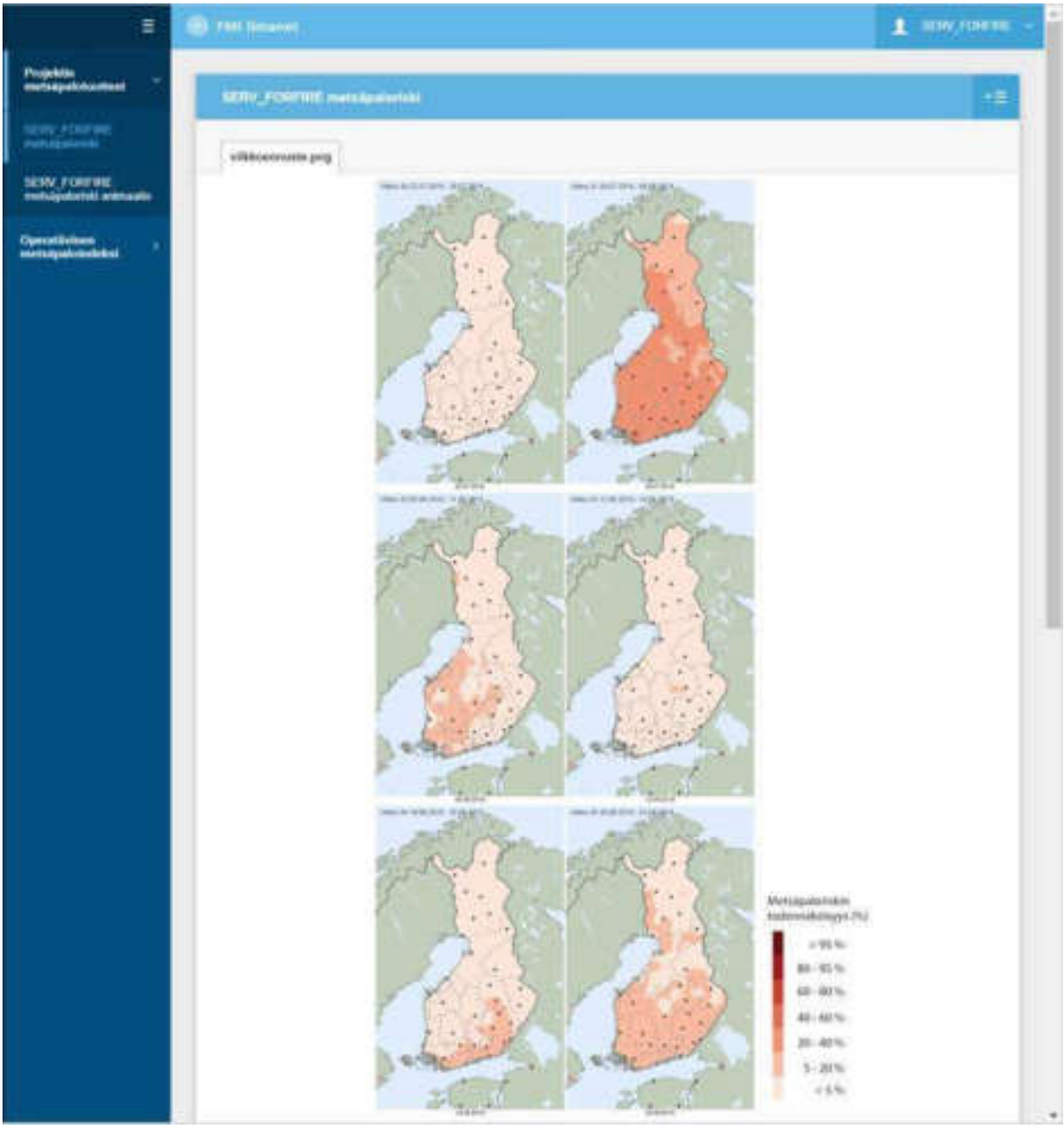

Figure 3 - The sub-seasonal forest fire risk outlooks and the user interface of the operational service; here presenting an example issued on July 19, 2019, the maps expresses the weekly probabilities of fire risk weather for the upcoming six weeks.

Although a detailed verification of the fire season 2019 forecasts was not possible due to the low sample of forecasts available a simple verification test was run to examine the performance of six week outlooks. The FFI forecasts for the weeks 1…3 during May-August 2019 have been tested against observed weekly FFI values (Fig. 4) for two regions: south and north of 65° latitude (Southern and Northern Finland). The correspondence between predicted and observed forest fire risk indicates that forecasts tended to underestimate the forest fire risk for both regions, very high fire risk (FFI>5) has not been forecasted at all. The accuracy of forecasts is lower after the first week.

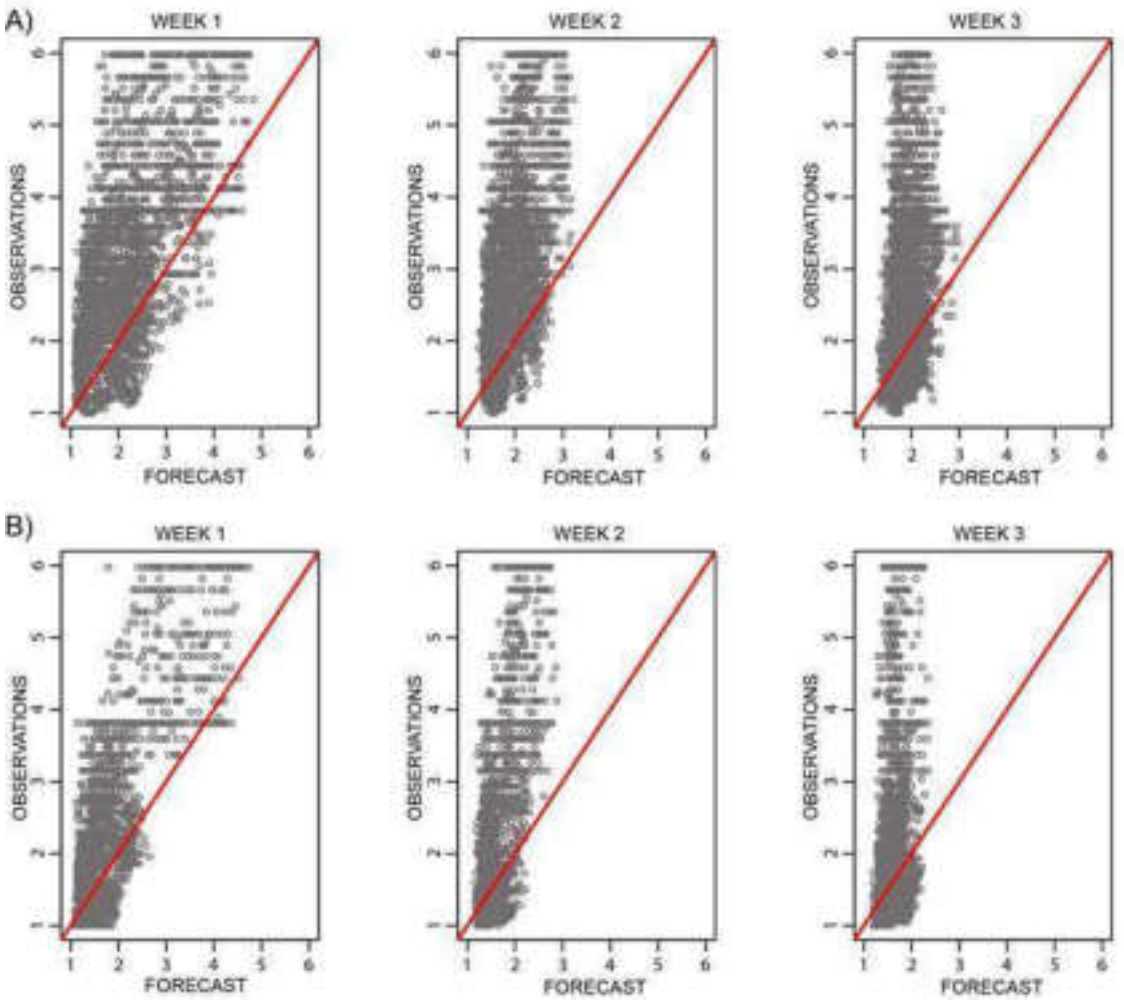

Figure 4 - Scatter-plots of observed and forecasted weekly mean FFIs for weeks 1…3 for (A) Southern Finland and (B) Northern Finland during May-August 2019.

The input parameters of the model, e.g. weekly means of 2m temperature, precipitation and relative humidity were also tested against observed values as shown in Fig. 5 (here shown the results for Southern Finland).

In summary to increase the reliability of developed and piloted sub-seasonal forest fire risk forecasts prototype for Finland further post-processing of the input variables is required, i.e. bias adjustment of input variables is needed to improve the skill of the model data. As the verification tests indicated the prediction skill of relative humidity is very low, thus for an improved version of statistical model we consider not using the relative humidity at all. Also, the comparison of weekly forecasted and observed FFI indicated an oversized role of temperature in the statistical model compared to precipitation, which should be equilibrated.

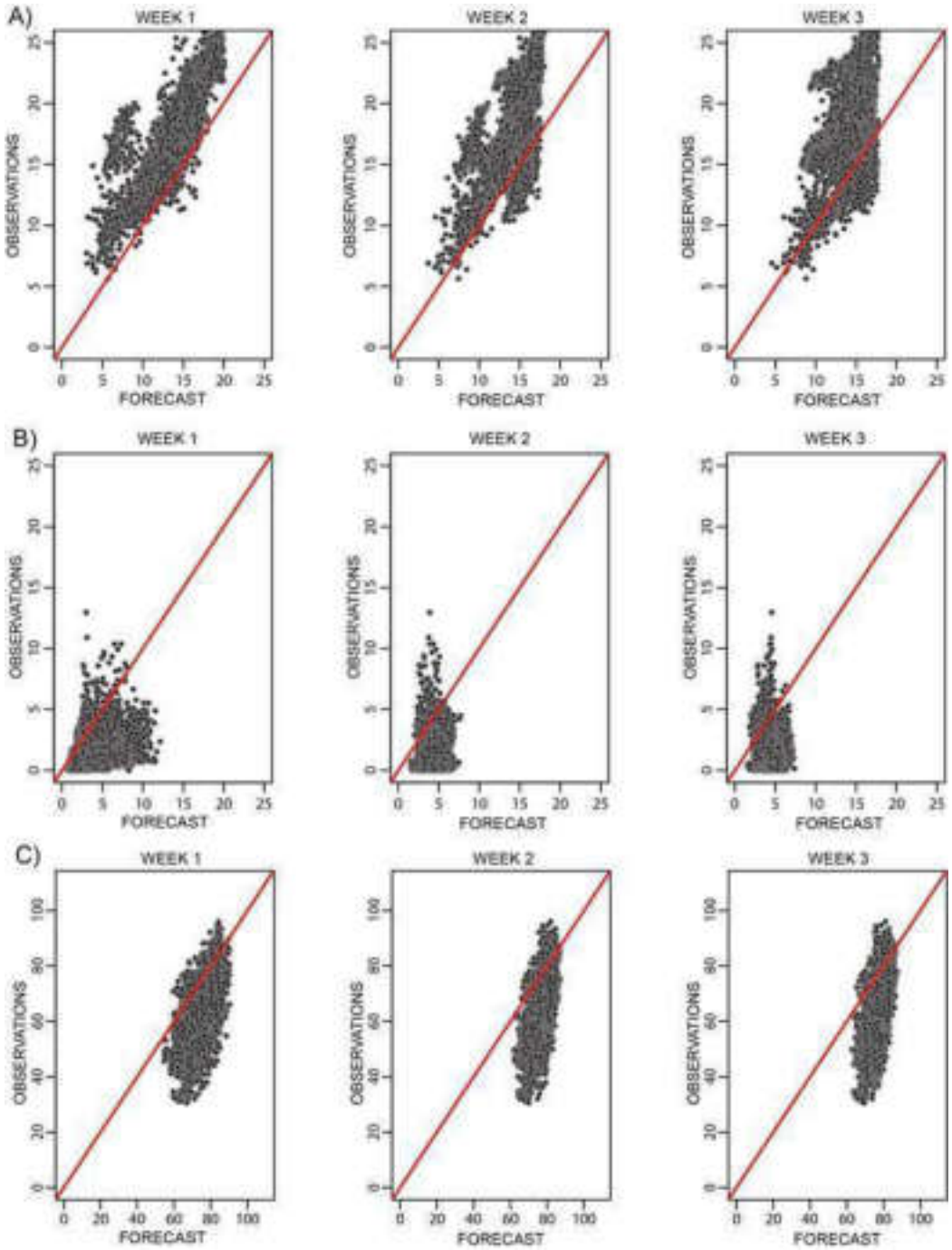

Figure 5 - Scatter-plots of observed and forecasted weekly mean (A) temperature, (B) precipitation and (C) relative humidity values for weeks 1…3 during May-August for Southern Finland.

Evaluation of the sub-seasonal forest fire risk outlooks by the users

The experience and value of six week forest fire risk outlooks for stakeholders was tested through a feedback survey at the end of pilot season. Responses were received both from AVI and the Rescues Services. In addition, a more detailed debriefing has been performed with AVI. Questions related to

(1) the benefit offered by the provided forecasts,

(2) how the information provided were taken into account in decision making,

(3) the improvements the stakeholders would prefer in the sub-seasonal forest fire risk forecast and

(5) their willingness to test the forecast in a second pilot season was addressed.

The users evaluated the sub-seasonal fire risk outlooks as very useful: “helped in making the plans more in advance than before” and “really helped in planning the survey flights in advance, for ex. the high probabilities from late July were predicted already in June, such as the amount of plains and workers needed for the survey flights”. Also, both of the users were willing to continue the pilot during the 2020 fire season and gave suggestions for improvements.

Improvements performed on the sub-seasonal forest fire risk forecasts

Several updates have been performed on the sub-seasonal forest fire forecast taking into account the verification results of the pilot season 2019 and of re-forecasts data (2008-2016) runs. According to verification results the model has underestimated the probability of sub-seasonal forest fire risk, the biases originating mainly from the poor prediction skill of relative humidity and partly precipitation. Air temperature indicated higher skill but with slight negative bias especially for the weeks 2, 3.

In order to increase the skill of the sub-seasonal forest fire risk forecasts the following improvements were performed:

(a) the developed statistical model was updated by eliminating relative humidity and by replacing the temperature values measured at 12 UTC used earlier in the model with the daily mean values and

(b) the systematic bias from raw model temperature output was reduced by bias adjustment.

The **developed model was updated** by applying a linear regression on the gridded observational daily mean 2 m temperature (T), daily accumulated precipitation (RR) and volumetric soil moisture (V) for the summer season 2003 to 2015 over Finland. As in the previous version, the one-week moving average of surface parameters was used in order to adjust the slower change of surface parameters compared to those of atmospheric parameters. The final statistical model is as follows:

The constants were determined by least-square fitting to the data: a = - 0.44060, b = 0.09586 and c = 7.64372. The FFI was determined, as previously, from the volumetric soil moisture.

The updated model was tested for the fire season 2019 and its results compared with the previously produced sub-seasonal fire forecast. Although the skill of the forecasts dropped after the 2nd week, the improved statistical model resulted in a higher correlation between the forecasted and observed fire risk.

To perform the **bias adjustment of daily temperature** values we tested two approaches: the model output statistics (EMOS) approach (Gneiting et al., 2005) and a simple mean bias correction method (Van Schaeybroeck and Vannitsem, 2018). According to the tests the simple bias correction method improved the bias better and it was selected to be used for adjusting the temperature bias in the fire risk calculation. Within this approach the bias was estimated as the difference between the forecasted and observed mean over the reference period; the estimated bias is used to adjust the real-time forecast. Bias was estimated using the re-forecast runs based on a 10-member ensemble and the ERA5 re-analysis data for the reference period 2000-2019. To correct the forecast value of a target day a rolling mean window of 7 days (centred, +-3 days) was applied. Estimated bias correction factors were applied to the middle day of the 1-week window for real-time forecasts. An example of calculated biases is shown in Fig. 6.

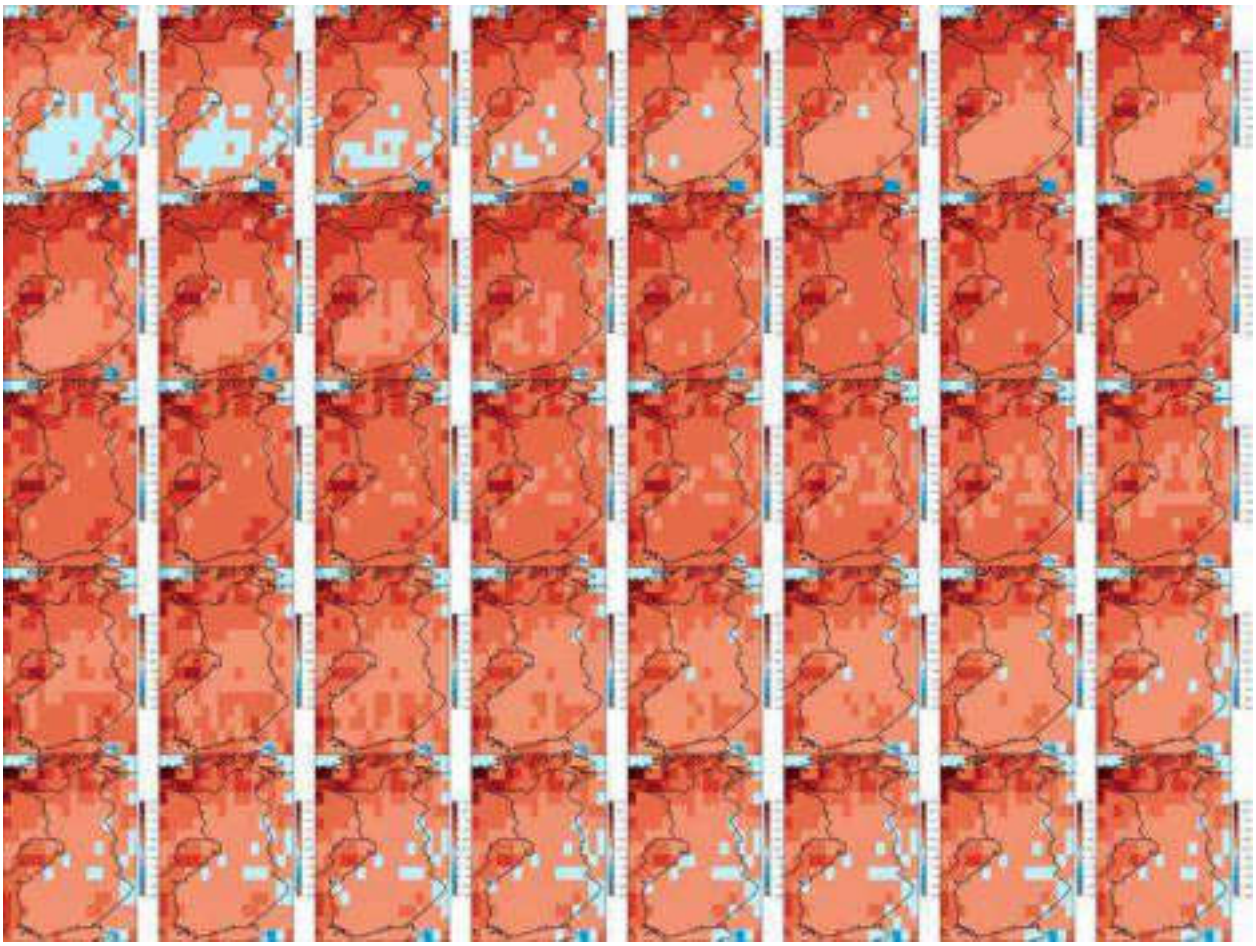

Figure 6 - Absolute bias calculated for July from ECMWF ENS re-forecasts and ERA5, daily values with 7-day rolling mean.

Bias adjustment of precipitation data would further improve the quality of forest fire risk forecasts. However, this process would require additional testing of various bias correction approaches that is not feasible within this project. Thus the raw model data was applied for

precipitation. Figure 7 shows weekly FFI values computed using as input non-bias corrected and bias corrected temperature values.

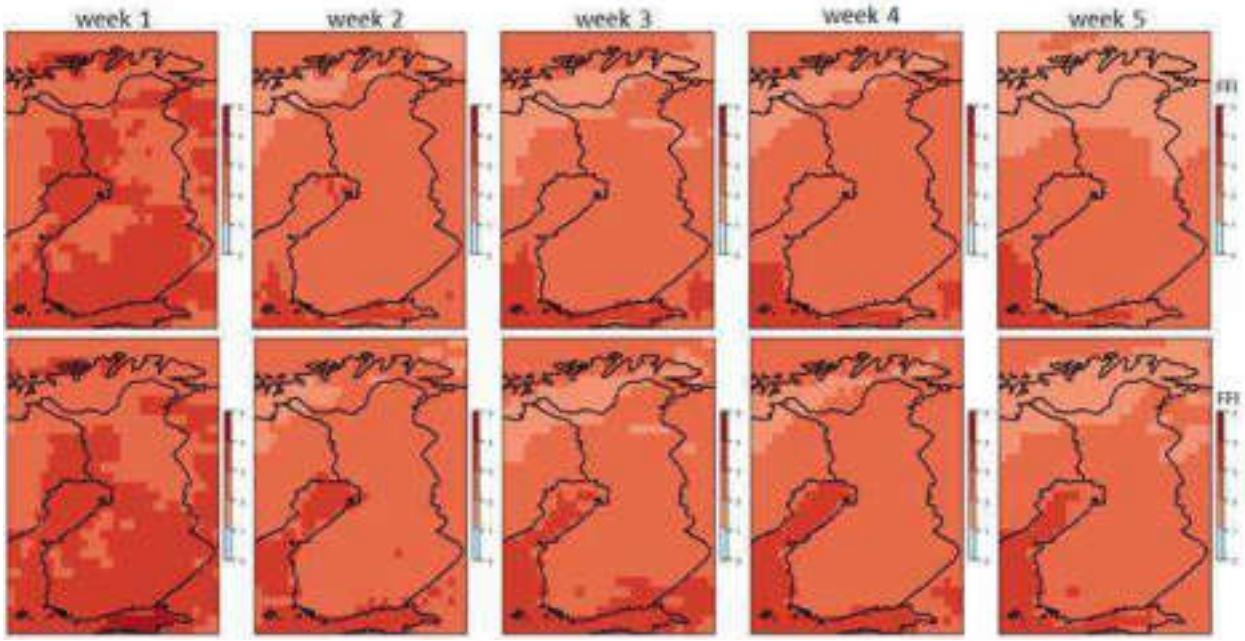

Figure 7 - Weekly FFI values initialized on 15.7.2019 computed from non-bias corrected (top) and bias-corrected (bottom) temperature values.

The updated model and the bias correction of input parameters were built into the operational service used for the production and dissemination of the six-week forest fire risk outlooks.

A new pilot phase of the improved sub-seasonal fire risk forecasts was launched in mid-April 2020 when the fire season started and will be tested by the users until the end of September. Following the second pilot season the performance of the improved forecasts will be assessed.

REFERENCES

- Gneiting, T., and M. Katzfuss, 2014: Probabilistic forecasting. Annu. Rev. Stat. Appl., 1, 125–151, https://doi.org/10.1146/annurev-statistics-062713-085831.
- Van Schaeybroeck B. and Vannitsem S., 2018: Postprocessing of long-range forecasts, in Statistical Postprocessing of Ensemble Forecasts edited by Vannitsem S., Wilks D.S. Messner J.W., DOI: 10.1016/B978-0-12-812372-0.00010-8

1.2 Iberian Wildfires during Hurricane Ophelia in October 2017

Contribution by FMI: Partanen T., Sofiev M.

In our case study, we examine Iberian forest fires during tropical storm Ophelia which took place in October 2017. Ophelia formed over the eastern Atlantic Ocean on the 9th of October and

dissipated over Europe on the 17th of October. Already-burning forest fires in Iberia accompanied by hot and dry air were further aggravated by Ophelia as it passed by off the coast of Portugal on the 15th of October. High winds from Ophelia fed and quickly spread wildfires resulting in an exceptional firestorm and devastation in Portugal and Spain. Fig. 8 illustrates a snapshot of a data animation of the forest fires in Portugal, Spain, and North Africa during the storm Ophelia roughly when it was closest to Portugal. The particularly strong and intensive forest fires in Portugal can be seen in the figure. The storm induced and carried a great deal of air pollutants in the form of a mixture of dust from the Saharan Desert, sea-salt from the Atlantic Ocean, and smoke from the Iberian forest fires into Europe and beyond. The pollutants worsened visibly the air quality in Europe, especially in the UK. We studied two aspects of the Iberian wildfires during Ophelia, namely the evolution of the emitted fire radiative power (FRP) and the dispersion of particulate matter (PM) emissions from the fires.

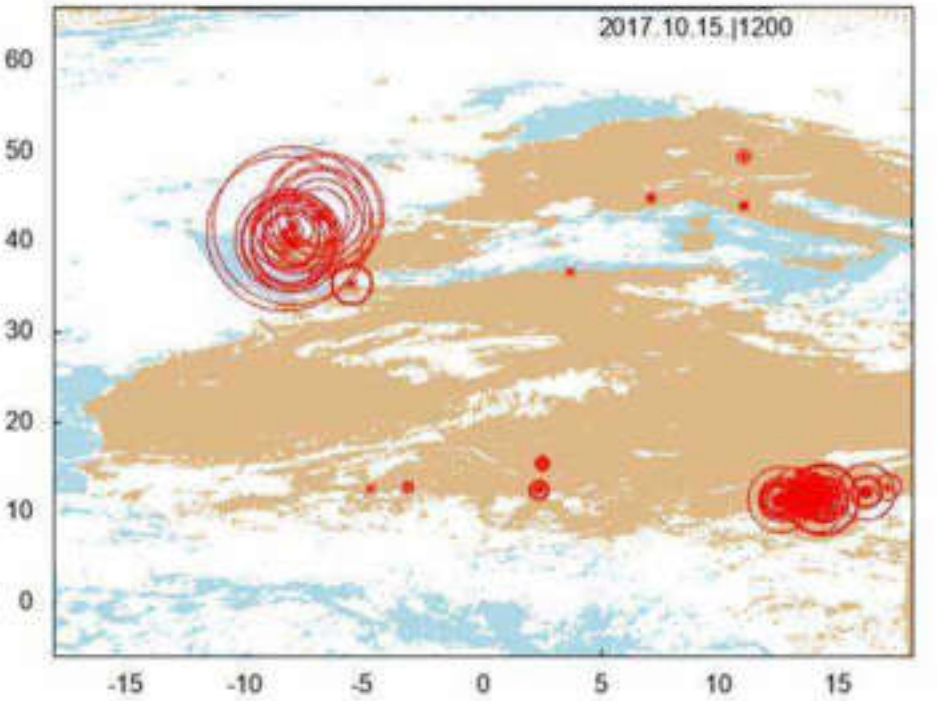

Figure 8 - Wildfires detected by SEVIRI on the 15th of October in 2017 at 12:00 UTC. The size of the red circle represents the amount of FRP a fire emits. White pixels are clouds.

In one of our two cases, we split Iberia into areas of size 1.5°×1.5° and investigated in detail the evolution of FRP emitted by each area. We exploit remotely-sensed data from SEVIRI instrument, which is onboard of the Meteosat Second Generation (MSG) geostationary satellite. It is positioned above Null Island located in the South Atlantic Ocean off the West coast of Africa at the point of 0° of longitude and latitude. The used data on FRP and cloud mask are observed by SEVIRI with a spatial resolution of about 3 to 4 km^2 and a temporal resolution of as high as 15 minutes.

Our interest in this case lies in the possibility to forecast future wildfires in Iberia by appropriately parameterizing for this purpose our developed fire prediction method that already shows promise in predicting African grassland fires reasonably well. As an example to demonstrate the FRP evolution in the Iberian area in 2017, we use here a larger area shown in Fig. 9, which covers

major part of the Iberian Peninsula. The area has a size of 6.5°×6.5° and its center point is located at 5.50°W 40.00°N in Spain. Figure 9 shows also the mean locations of fires for three different years 2010, 2017, and 2018. The mean locations for 2010 and 2018 are based on data over a period of six months from April to September, while for 2017 is based on data over the full year. Since they are within about half a degree from each other, the fires seem to concentrate in a rather small area in Iberia. Figure. 10 shows FRP maxima values and their monthly averages emitted by the area for the full year 2017 on cloudless or nearly cloudless days, *i.e.,* the true, unmasked values. Figure 11 shows diurnal FRP patterns from fires during the close proximity of Ophelia to Iberia. The FRP patterns in the figure resemble the ones that arise from the African grassland fires, which makes us cautiously optimistic that predicting Iberian forest fires may be doable at least in extreme cases like Ophelia. However, even though FRP correlates with weather conditions, the ignition of wildfires does not. African grassland fires in the neighbourhood of south-central Africa are presumably agricultural type, which are constantly ignited on a daily basis and have a high incidence. In the case of these type of fires, our predictions show a strong correlation between observed and predicted daily fire radiative energies of different areas sized 1.5°×1.5°. Unfortunately, when it comes to forest fires, for example, they are ignited much more sporadically and thus, they do not necessarily occur on a daily basis within a specified area, and they typically also have a low incidence. Therefore, this inconvenience makes it practically impossible to make reasonable day-by-day predictions in the case of forest fires.

Figure 9 - The FRP area sized 6.5°×6.5° within the red perimeter located at 5.50°W 40.00°N.

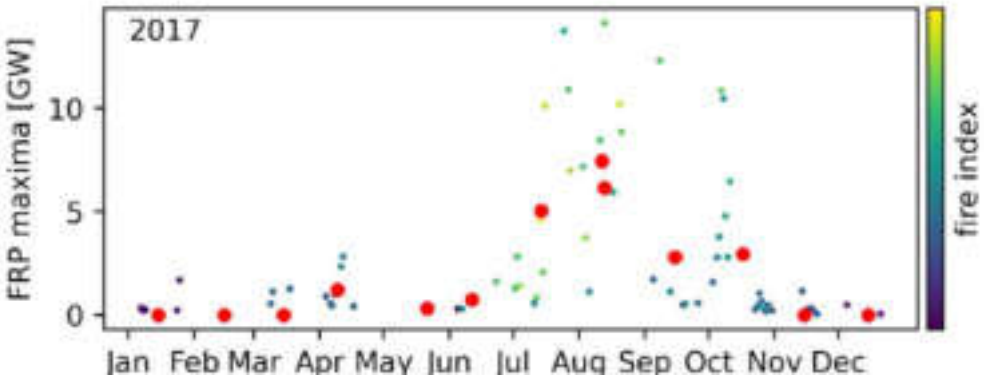

Figure 10 - Values for FRP maxima observed by SEVIRI in 2017. Each point represents a value on a cloudless or nearly cloudless day. The colorbar shows the value of the fire index. The ERA5 re-analysis data are used for the meteo. The red dots represent the monthly averages, apart from the topmost one at the maximum, which depicts an average of a few neighbouring values.

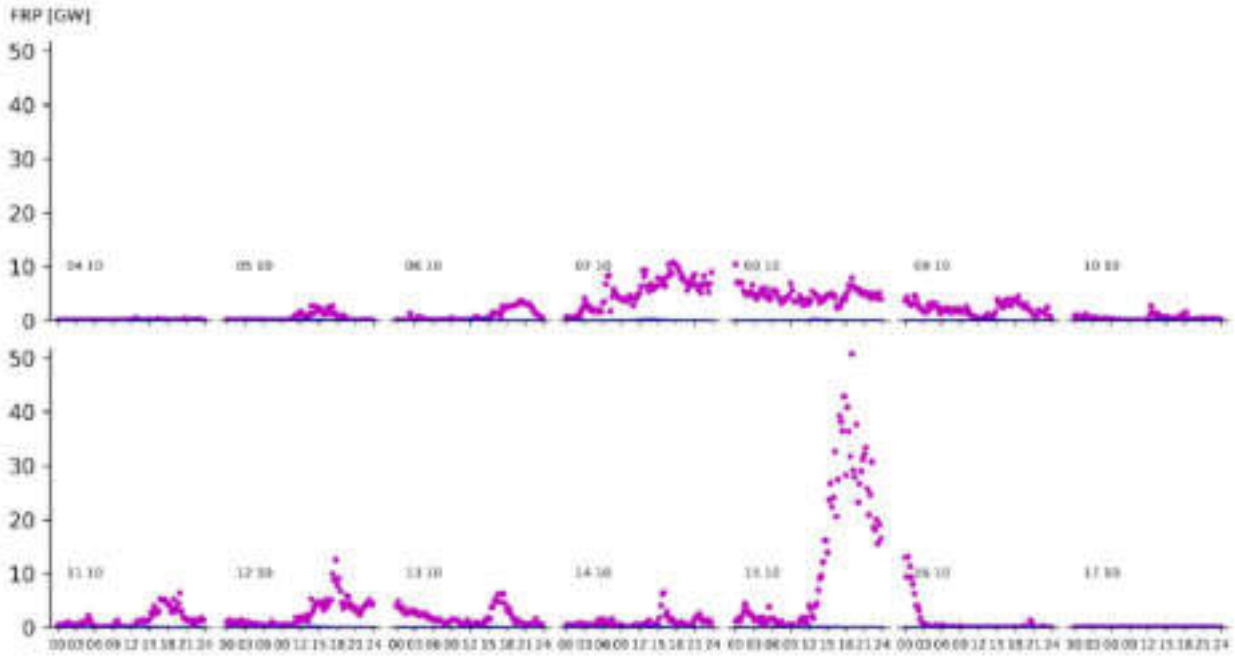

Figure 11- FRP emitted by the 6.5°×6.5° sized area at 5.50°W 40.00°N in the Iberian Peninsula between the 4th and 17th of October 2017 observed by SEVIRI. The vertical axis is in units of GW and the horizontal one is the local time of the coordinate point in the 24-hour clock format. The days from the 13th to the 17th are cloudy and the rest of the days either a little bit cloudy or cloudless. Notice the strong power peak on the 15th day despite the area is heavily covered by clouds. Both the 16th and 17th days, especially the latter one, are rainy days

In the other case, we made two simulation runs whose methodology builds upon the FMI tools IS4FIRES (Integrated System for wild-land fires, http://is4fires.fmi.fi) and SILAM (System for Integrated modeLling of Atmospheric coMposition, http://silam.fmi.fi). The simulations were made with two different fire datasets: one for SEVIRI instrument and one for MODIS one. The two identical Moderate-resolution Imaging Spectroradiometer (MODIS) instruments are on-board NASA's Terra and Aqua near-Earth orbiting satellites. MODIS instruments have a spatial resolution of about one kilometer squared at nadir and together they scan nearly all locations

over the whole globe up to four times a day. The temporal resolution of MODIS is very low and ill-defined, unlike the one of SEVIRI which is high and well-defined. Figures 12 and 13 illustrate snapshots of a fire-induced particulate matter (PM) concentration simulation over Europe. The simulation exploited SEVIRI FRP data and were performed by using the SILAM model. The figures represent, respectively, the concentration distributions on the day Ophelia hit the coast of Portugal and two days later after it had subsided over Norway. Ophelia transported the smoke plumes from the fires in Iberia towards northwest Europe in the direction of its trajectory. Plumes with relatively high PM concentrations were quickly transported over large distances across Europe all the way far to Russia. The total disagreement between the simulated emissions is about 20 % between the two sets of fire sources, SEVIRI and MODIS. The discrepancy may be explained by the differences between the two instruments in their temporal resolutions and sensitivities to detect fires. The simulated PM emissions may be too low, since many of the fires are covered by clouds and thus undetected by satellites.

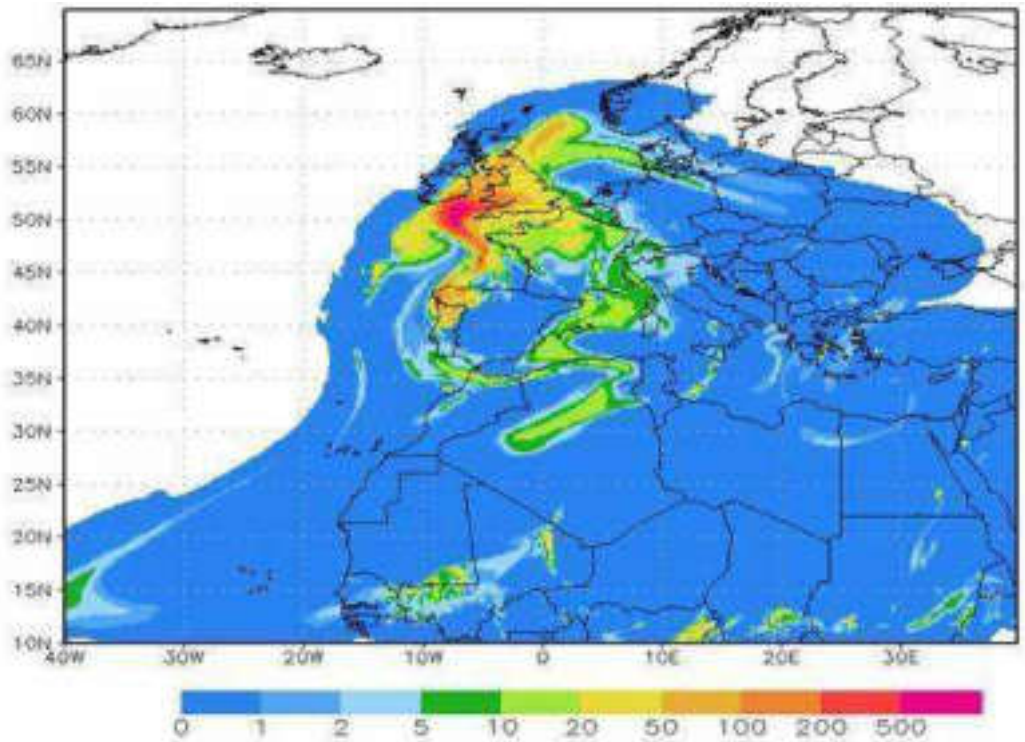

Figure 12 - Concentration of PM 0.05 - 20 µm in units of µg/m3 based on FRP observed by SEVIRI on the 15th of October in 2017 at 12:00 UTC.

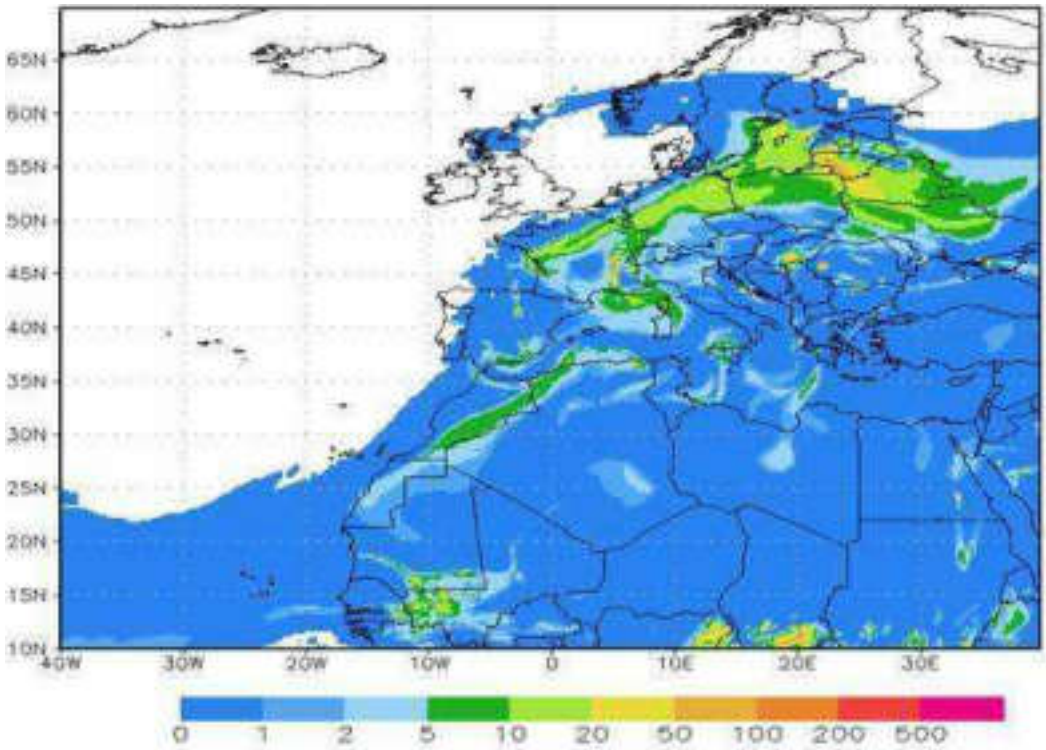

Figure 13 - Same as Fig. 12, but for the 17th of October in 2017 at 12.00 UTC.

1.3 Trend Assessment of Drought Condition for the Tuscany region pilot area

Contribution by CNR-IBE: Pasqui M., Quaresima S., Di Giuseppe E.

We propose a trend test for the different classes of drought risk based on the Poisson process (Di Giuseppe et al., 2019). In the framework of the time series of SPEI values calculated at a specific time scale and for a given month, we can consider the inter-arrival times—years in this case—between drought episodes as independent and identically distributed. Consequently, the point process becomes a counting process and the natural distribution used to describe such a counting process is the Poisson distribution. Furthermore, if the arrival rate does not remain constant through time, then it follows a Non-Homogeneous Poisson Process (NHPP). We consider the use of a special case of the NHPP: the power law process.

An advantage of using a counting process approach for testing the trend, in the case of those drought indexes that allow for thresholds definition, is the possibility of distinguishing the results among different classes of risk. This is particularly useful for risk management, such as the management of water resources. Thus, the characterization of the type of drought risk, that is to know whether in a specific area the increasing of drought episodes regards the extreme or the moderate ones, is intrinsically important. We also compare the NHPP method with a standard one: the Mann-Kendall.

We used the CRU TS v.4.03 gridded time-series dataset, released by Climatic Research Unit, University of East Anglia and applying a dry mask with a 3 mm monthly threshold that guarantees from errors in the SPEI computation.

The phase of data preparation for trend analysis is composed of two parts: (1) the computation of SPEI time series from precipitation and evapotranspiration data at 3-, 6-, 12- and 24-month scale of aggregation; and (2) the sub-setting of SPEI time series for each month of the year. The final output of this phase is represented by 48-time series resulting from the 4 aggregation scales (3-, 6-, 12- and 24-month) multiplied by the 12 months of the year (Figure 14). Thus, for each month, we have a time series of 118 values corresponding to the number of years in the time window 1901–2018. Let us label the SPEI time series as SPEI-3, SPEI-6, SPEI-12, and SPEI-24 according to the scale of aggregation such that, for example, the time series of SPEI at 6-month for March is briefly indicated as SPEI-6 March.

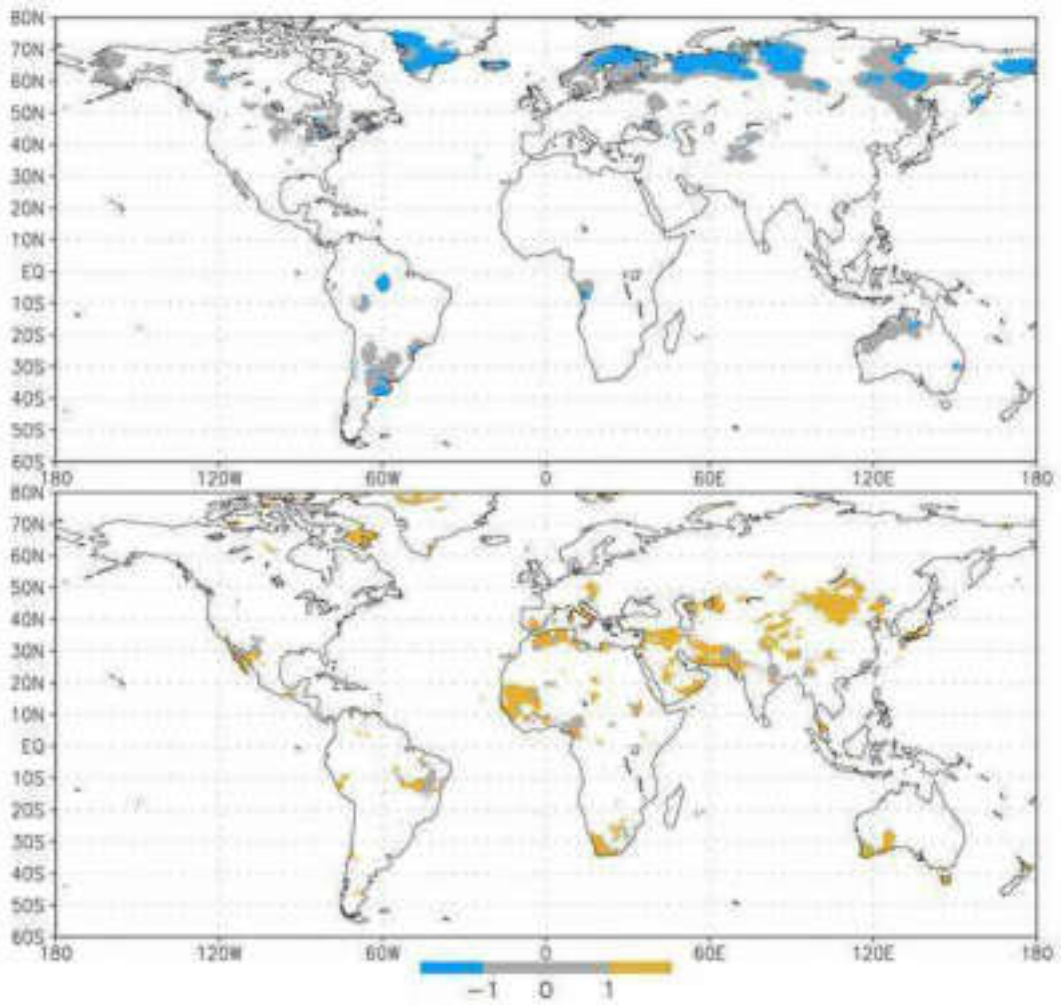

Figure 14 - Spatial distribution of cases where the M-K gives a negative (top) and positive trend (bottom) and the response of the NHPP test on the same areas for SPEI-6 March: In the top panel, the M-K negative trend cases are blue and grey, while the NHPP non-significant trends are in grey.

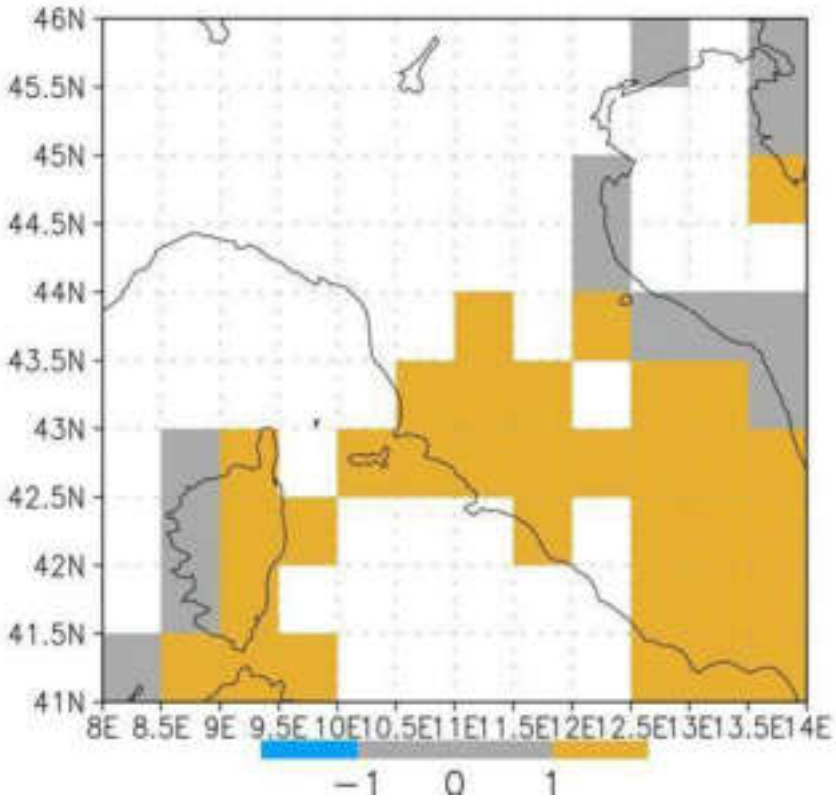

Figure 15 - Same as Fig.14 - bottom, but for the pilot target area of Tuscany region.

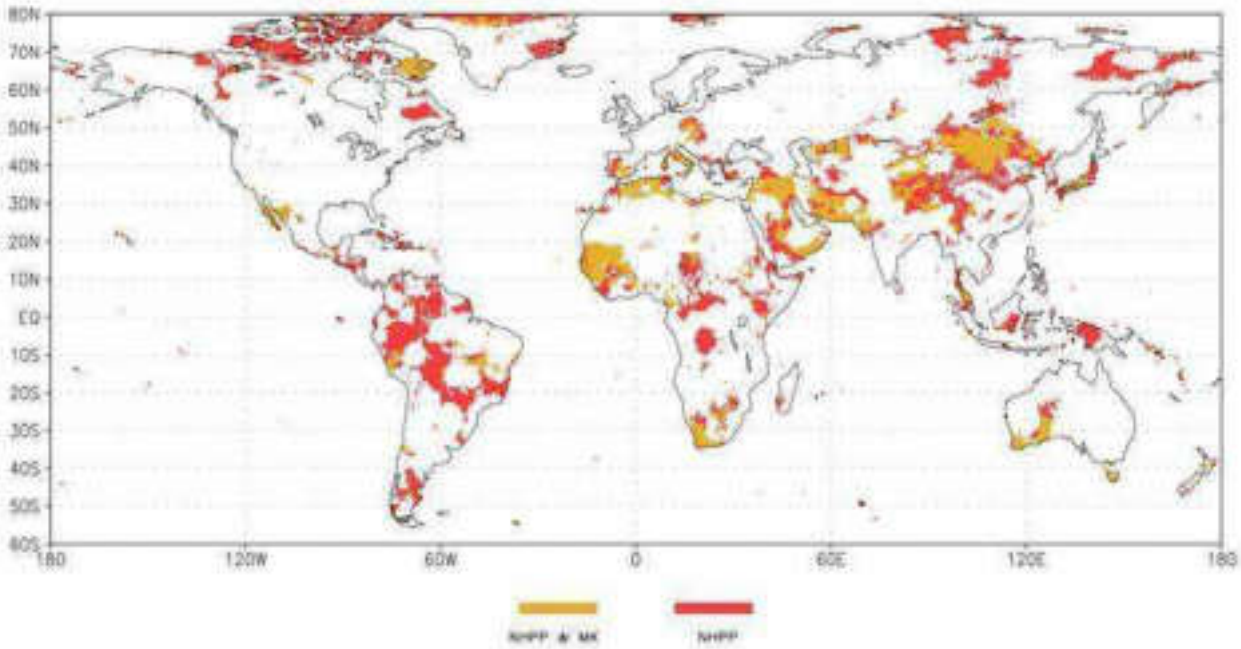

Figure 16 - Areas of the globe interested by an increasing trend of drought episodes identified by SPEI-6 for the month of March. Significant positive trend: (1) only for NHPP (red areas); and (2) for NHPP and M-K (yellow areas).

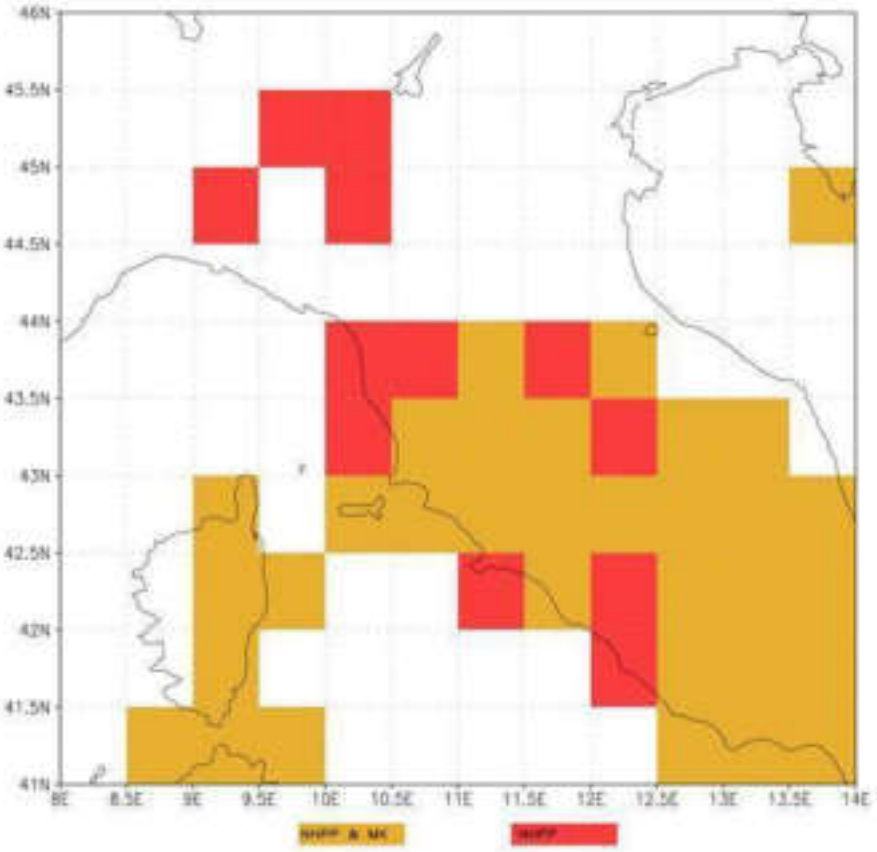

Figure 17 - Same as in Fig.16, but for the pilot target area of Tuscany region.

1.4 A drought empirical forecasting system for the Mediterranean basin.

Contribution by CNR-IBE: Pasqui M., Magno R., Quaresima S., Di Giuseppe E.

A drought-monitoring and forecasting system, developed for the Tuscany region, was improved in order to provide a semi-automatic, more detailed, timely and comprehensive operational service for decision making, water authorities, researchers and general stakeholders.

Figure 18 - An example of the Drought Observatory web GIS portal available via: https://drought.climateservices.it/en/.

The forecasting system is based on an empirical approach to predict meteorological drought using the SPI 3, a few months in advance from large-scale observed climate indices. The forecast's window (25°–65° N; 20° W–45° E) has a spatial resolution of 0.5°. This seasonal forecast empirical system adopts a physically based statistical approach which uses a multivariate regression (MR) model to estimate future anomalies. The entire structure is extensively described in Magno et al., 2018. As an example, here is the issued forecast of SPEI index for OND 2019 season.

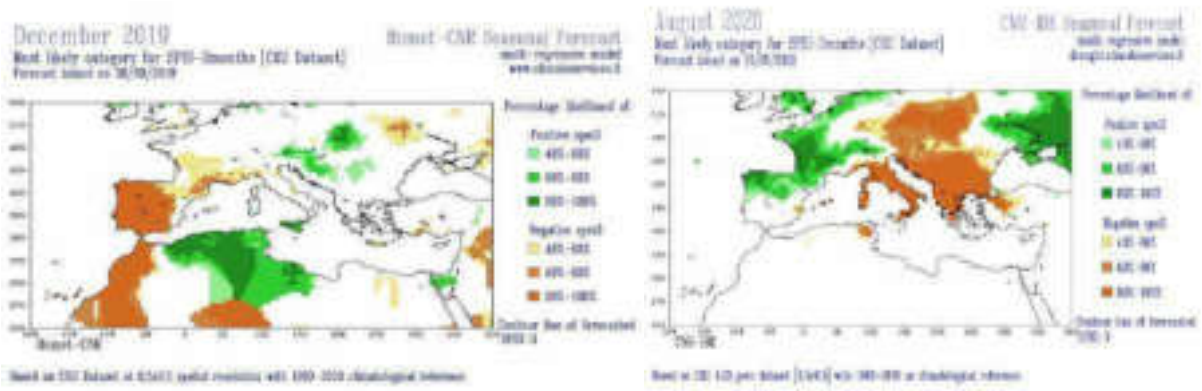

Figure 19 - Two examples of the empirical seasonal forecast of SPEI index issued in late September for OND 2019 and in late May for JJA 2020. These forecasts are available via: https://drought.climateservices.it/en/.

The empirical drought forecasting system is thus operational for both SPI and SPEI indexes (on quarterly timescale) on a monthly basis on a wide region covering Europe, the whole Mediterranean Basin and north Africa. An overall assessment phase of the reliability of this system is now started and it is currently underway. Using typical forecasting skill scores the aim of the current activity is to evaluate reliability performances of the empirical system.

1.5 A drought Climate Service system for Central Europe and Mediterranean basin

Contribution by CNR-IBE: Magno R.

The Drought Observatory (DO) Climate Service, developed by the Institute for Bioeconomy of the Italian CNR, is operational from 2019. The DO integrates ground-based and satellite data through open source solutions and interoperable services to produce vegetation and rainfall indices able to follow the occurrence and the evolution of a drought event.

In particular, the coupled rainfall based and satellite-derived monitoring system allows the assessment of vegetation moisture and temperature conditions at different spatio-temporal scales.
An interoperable Spatial Data Infrastructure (SDI) that include a geospatial Data Cube, allows the download, storage, access, analysis, and geoprocessing of remote sensing and climatic data and the dissemination of an updated and customizable information, that facilitates the transfer of research know-how to operational applications.
Due to the extreme flexibility of the System, new procedures of analysis, new indices and areas of interest can be easily integrated with a relatively low development workload.
In the last months, in fact, two implementations were done:

1. API to calculate basic geographic statistics (mean, minimum, maximum, standard deviation, number of pixels, 25° and 75° quantiles) of a defined polygon or a specific pixel, for each time period (https://drought.climateservices.it/wp-admin/post.php?post=585&action=elementor);

2. the initial geographic window of the vegetation indices was extended from the central Mediterranean to the western part of the Basin and Central Europe.

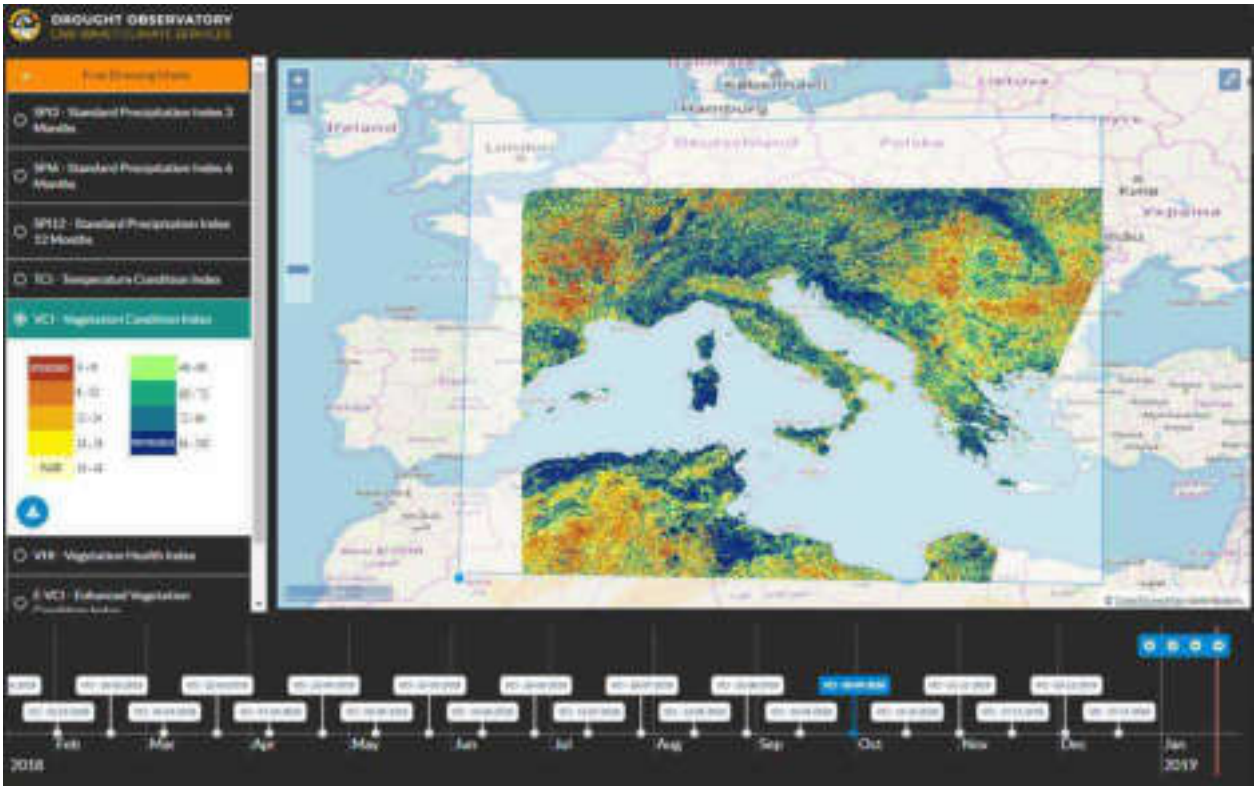

Figure 20 - An example of the initial geographic window for TCI, VCI, VHI and E-VCI vegetation indices.

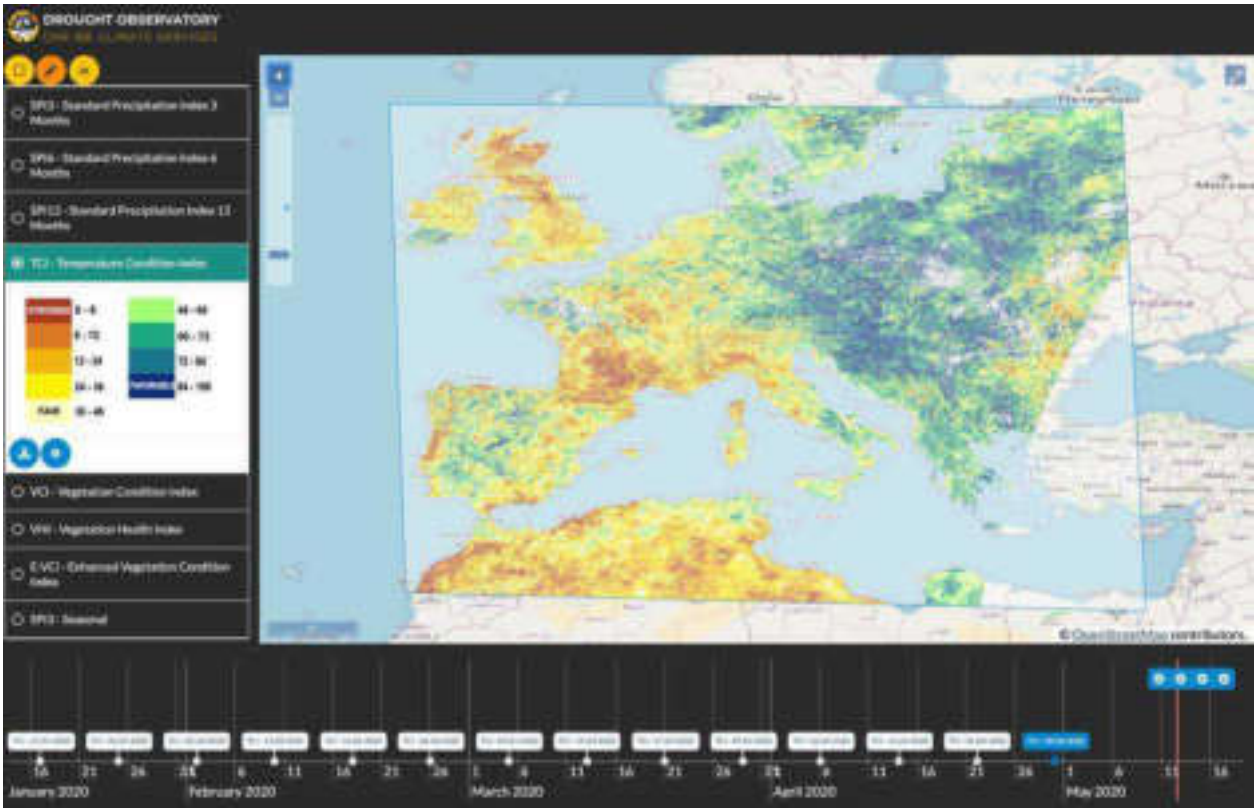

Figure 21- An example of the current geographic window for TCI, VCI, VHI and E-VCI vegetation indices.

REFERENCES

- Di Giuseppe, E., Pasqui, M., Magno, R., & Quaresima, S. (2019). A Counting Process Approach for Trend Assessment of Drought Condition. Hydrology, 6(4), 84.
- Magno, R., De Filippis, T., Di Giuseppe, E., Pasqui, M., Rocchi, L., & Gozzini, B. (2018). Semi-automatic operational service for drought monitoring and forecasting in the Tuscany region. Geosciences, 8(2), 49.

1.1 Emission factors on the case study "Metaponto Natural Reserve"

Contribution by CNR-IRET: Calfapietra C., Pallozzi E., Nestola E., Caccavale L., Guidolotti G.

Monitoring ecosystem properties in relation to the fire occurrence and measuring vegetation fire emission were the main activities carried out by CNR IRET.

The case study area was located at the Metaponto Natural Reserve, Basilicata Region, South of Italy. The site was selected for both its proneness to fire and its proximity to a burned area, similar in both vegetation and topographic complexity. Five plots were sampled for the field campaign on 3rd and 4th August 2019 (Fig. 22).

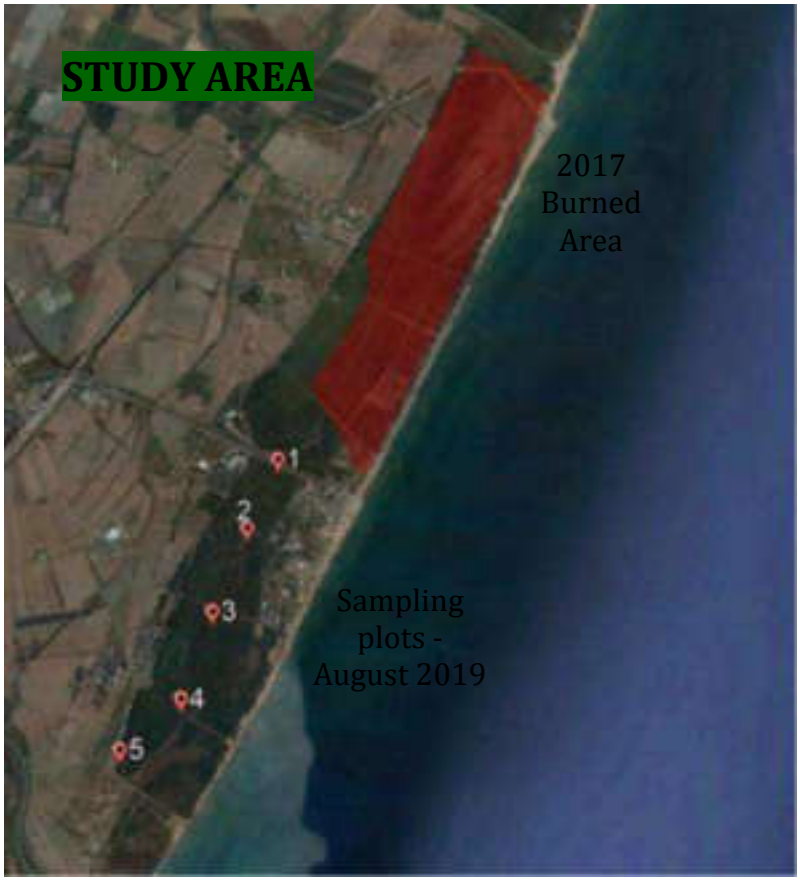

Figure 22 - Study area, Metaponto Natural Reserve, Basilicata Region (Italy). Field sampling locations are displayed in red.

The field campaign was aimed to:

- Characterize the case study area, in terms of plant specific composition and abundance
- Collect biomass samples for the analysis of the emission during the fire.

Regarding the characterization of the area, parameters as woody species, mean height, mean diameter and plot density were quantified (Figure 23).

Sampling Plot	Woody Species	Mean height	Mean diameter	Plot Density
1	**Dominant Layer**			980 trees/ha
	Pinus halepensis	9 m	20 cm	
	Ecualyptus camaldulensis	9 m	10 cm	
	Understory			
	Juniperus communis	Rare		
	Pistacia lentiscus	Rare		
2	**Dominant Layer**			477 trees/ha
	Casuarina equisetifolia	3.5 m	5 cm	
	Understory			
	Juncus acutus	Rare		
	Pistacia lentiscus			
3	**Dominant Layer**			980 trees/ha
	Pinus halepensis	3 m	12 cm	
	Understory			
	Pistacia lentiscus	Rare		
4	**Dominant Layer**			1000 trees/ha
	Pinus halepensis	2.5 m	3.5 cm	
	Acacia farnesiana	3 m	5 cm	
	Understory	Missing		
5	**Dominant Layer**			490 trees/ha
	Pinus halepensis	10 m	30 cm	
	Understory	Missing		

Figure 23 - Characterization of the study area at Metaponto Natural Reserve, Basilicata Region (Italy).

The studied species were four trees (*Pinus halepensis*, *Eucalyptus camaldulensis, Casuarina equisetifolia, Acacia farnesiana*) and two shrubs (*Pistacia lentiscus, Juniperus communis*). Needles/leaves together with small woody branches were separately collected at the 5 sampling plots in the study area. Needle/leaf litter were similarly sampled in the same areas.
Gases and particles emitted from vegetation fire were analysed using: 1) a combustion chamber, which continuously samples emissions throughout the different phases of a fire (pre-ignition, flaming and smouldering) and 2) a scanning electron microscopy coupled with energy-dispersive X-ray spectroscopy: SEM/EDX. The aim was an accurate determination and parameterization of the emission factors of various compounds such as CO_2, CO, CH_4, particulate matter (PM) and volatile organic compounds (VOCs), allowing the analysis of the different combustion phases of various plant tissues in different species.

Combustion test have been performed on the biomass sampled in Metaponto in August 2019 using a customized combustion chamber. CO_2, CO and O_2 concentrations, gas and biomass temperatures were measured in real-time with an MRU gas analyser. Several BVOC concentrations were detected with a PTR-MS that was connected to the gas exhaust of the chamber. The weight for the biomass fuel was measured in real-time as well. One cartridge for each combustion phase (pre-ignition, flaming, smouldering) were taken to be analysed after with a GC-MS. PTR-MS in fact can give real-time information on many VOCs but it cannot separate isobaric compounds. GC-MS on the contrary can give only one result for each sampling, but with

this technique we can obtain more qualitative information. For these reasons, the two methods are complementary. In the following table (Table 1) we show the data obtained from each combustion experiment. *Heat peak* is the maximum temperature measured inside the biomass. *O_2 min* is the minimum O_2 concentration (%) detected. CO_2 and CO data are expressed as gram emitted for each Kg of biomass burned. We also noted the percentual of CO_2 and CO emitted on each phase.

	Litter	Litter 1	Litter 2	Litter (lichens)	Juniperus communis	Pinus halepensis
Heat Peak	699.1	649.4	783.2	582.6	667.0	653.0
O_2 min	19.6	17.8	17.8	17.5	17.7	18.4
CO_2 g Kg^{-1}	681.8	1979.6	1299.2	1572.2	892.3	1343.5
P %CO_2	0%	2%	0%	0%	0%	2%
F %CO_2	66%	74%	96%	75%	78%	65%
S %CO_2	34%	24%	4%	25%	22%	33%
CO g Kg^{-1}	89.4	120.8	95.6	74.2	109.3	105.5
P % CO	0%	16%	4%	1%	14%	11%
F % CO	18%	31%	53%	32%	33%	40%
S % CO	81%	53%	42%	67%	53%	49%
Pre-ignition duration	02:05	04:56	02:53	01:29	04:16	02:53
Flaming durations	01:57	02:57	04:52	02:46	01:27	02:45

Table 1: out of burning experiments (P=pre-ignition, F=flaming, S=smouldering).

Gas emissions dynamics were also studied during the different combustion phases. Studying the alternate of gaseous compounds emissions during the fire events is a crucial issue to fully understand the fire events dynamics. Here we describe one single case of *Pinus pinea* combustion of samples harvested in Metaponto during the summer of 2019 (Figure 24). About 110 grams of biomass were put on the burning plate, and only 8% of biomass remained uncombusted. The pre-ignition phase was characterized by the sole CO emission and lasted about 4 minutes. At the end of this phase, when small firebrands started to appear, CO_2 immediately raised, characterizing the flaming phase. In this phase temperature of both biomass and exhaust gas temperatures raised, reaching a maximum of 753.9 and 150.9°C respectively. O_2 during flaming

was consumed, acting as oxidant of the biomass fuel that was quickly depleted as shown in the weight graph (Figure 25). Methanol, the most volatile among the analysed compounds, was the first to be released, followed by benzene and toluene (Figure 26). These VOCs were released starting with the pre-ignition phase and continuing over the whole flaming phase, lowering at the beginning of the smouldering. Many more compounds have been detected for real-time analyses, and a cartridge for each phase has been collected for punctual VOC determinations to be analysed with a GC-MS. Data are still under analyses.

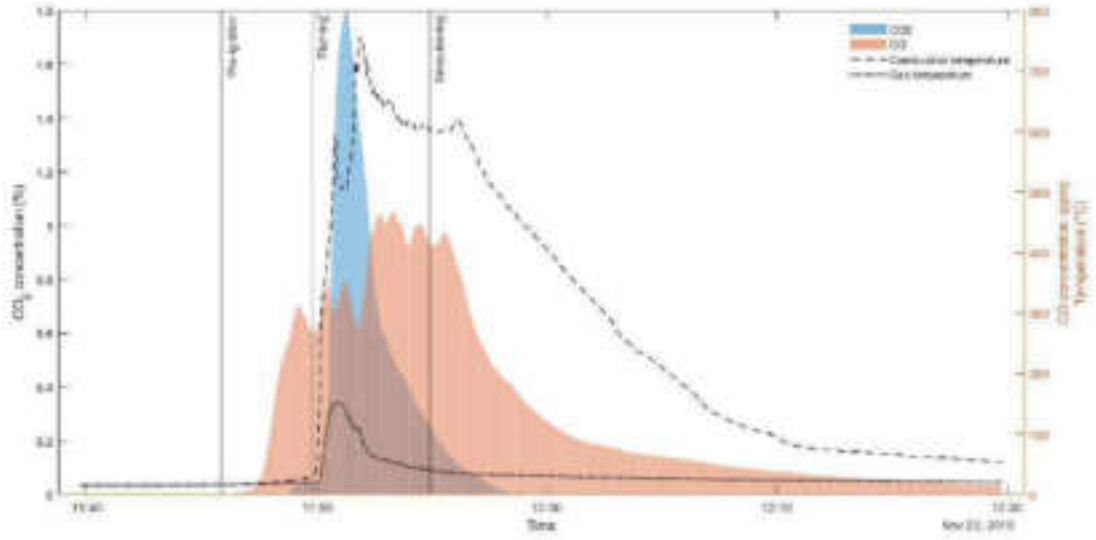

Figure 24 - CO (ppm) (blue area) and CO2 (%) (red area) concentrations, biomass (dashed line) and exhaust gas temperatures (dotted line) during the combustion of about 110g pine biomass.

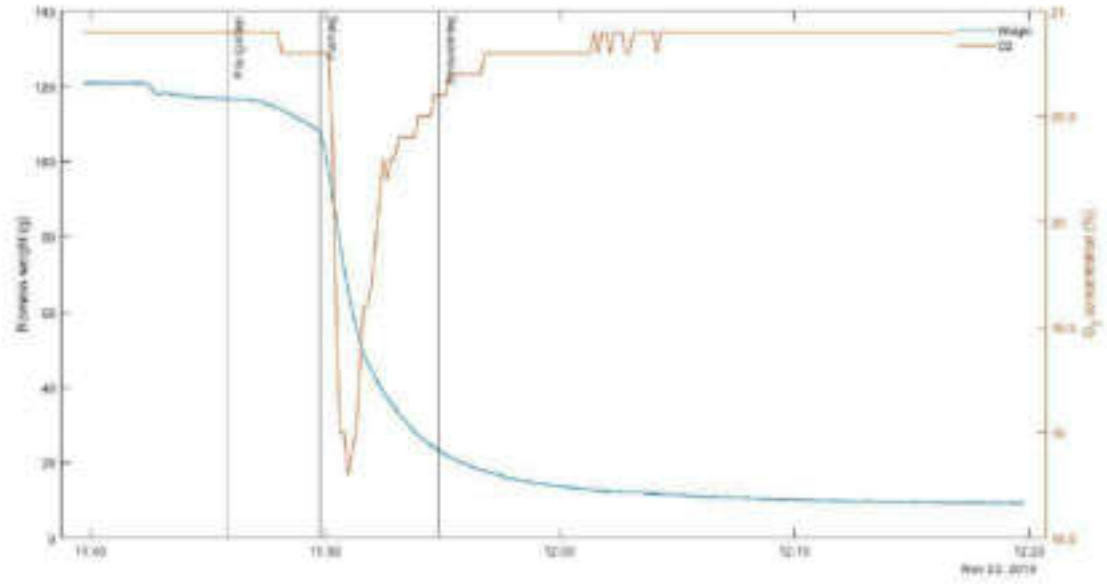

Figure 25 - O2 % (red line) and Weight (g) (blue line) during the combustion of about 110g pine biomass.

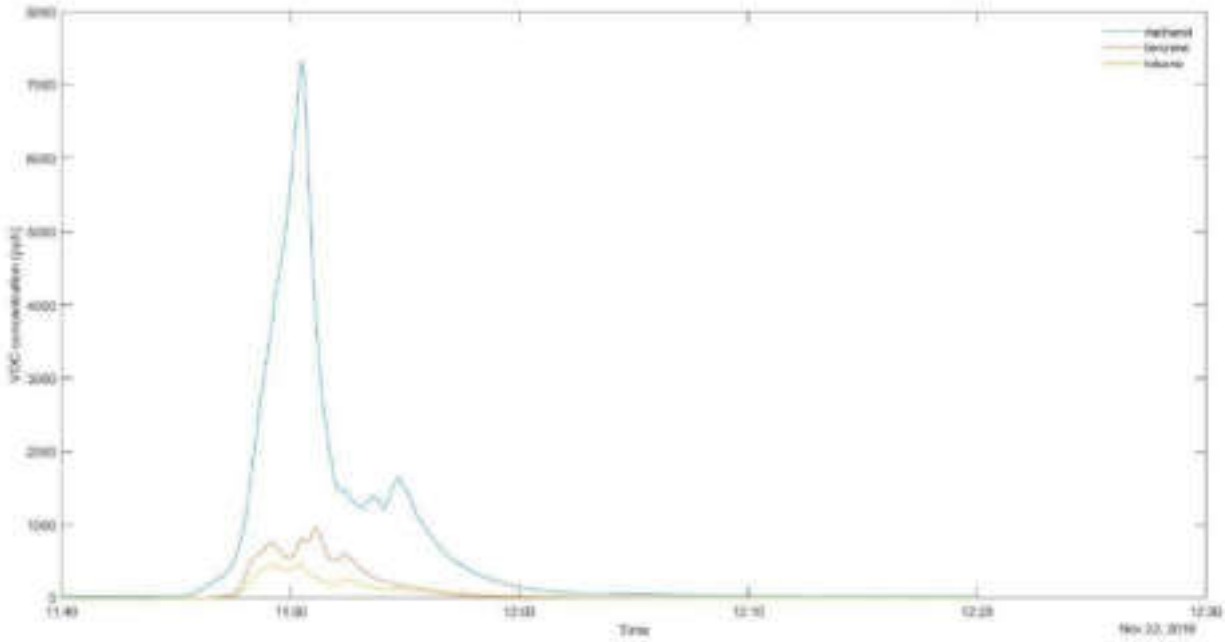

Figure 26 - Methanol, Benzene and Toluene concentrations (ppb) during the combustion of about 110g pine biomass.

As PM is one of the significant emissions from forest fire, we were aimed to calculate the total amount of particulate emitted and the relative size fraction.

During the combustion experiments, an isokinetic sampling line was used for the collection of PM on filters (nitrocellulose filters, 0.2 µm porosity). To achieve isokinetic sampling of PM, the flow rate through the sampling system was adjusted to the same flow rate of the fluid moving inside the exhaust chimney using a needle valve placed between the filter and the sampling pump (Pallozzi *et al.*, 2018). Filters were used as substrate to perform a quali-quantitative analysis of PM through scanning electron microscopy (SEM; Phenom ProX, Phenom-World, The Netherlands). 60 random images with a scan size of 150 × 150 µm were acquired for each filter, at a resolution of 1024 × 1024 pixels. SEM images were analysed with Gwyddion software, in order to obtain the number and the dimensions of particles originating from the combustion (Nečas and Klapetek, 2012).

Figure 27 shows the total amount of PM for litter in three different areas. No differences were found comparing Area 2 and Area 3, while lower values are evidenced for Area 1.

Similarly, branches and leaves filters follow the same pattern with lower PM density for the species in Area 1 and higher values for Area 2 and 3 (Figure 28). The highest number of particles was found for *Acacia farnesiana* in Area 4. Considering that the particle density of *Acacia* could be twice the amount of other species, further investigations on species leaf traits differences are required (Sgrigna *et al.*, 2020).

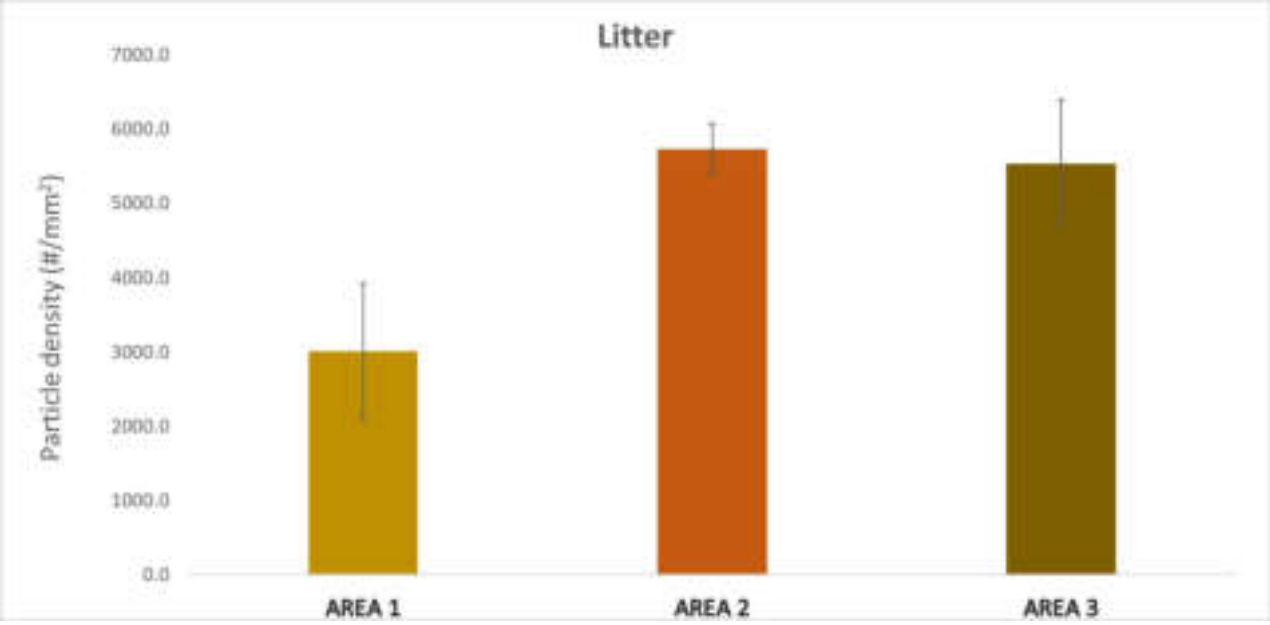

Figure 27- Total particle density across study areas for litter presented as number of particles on filter.

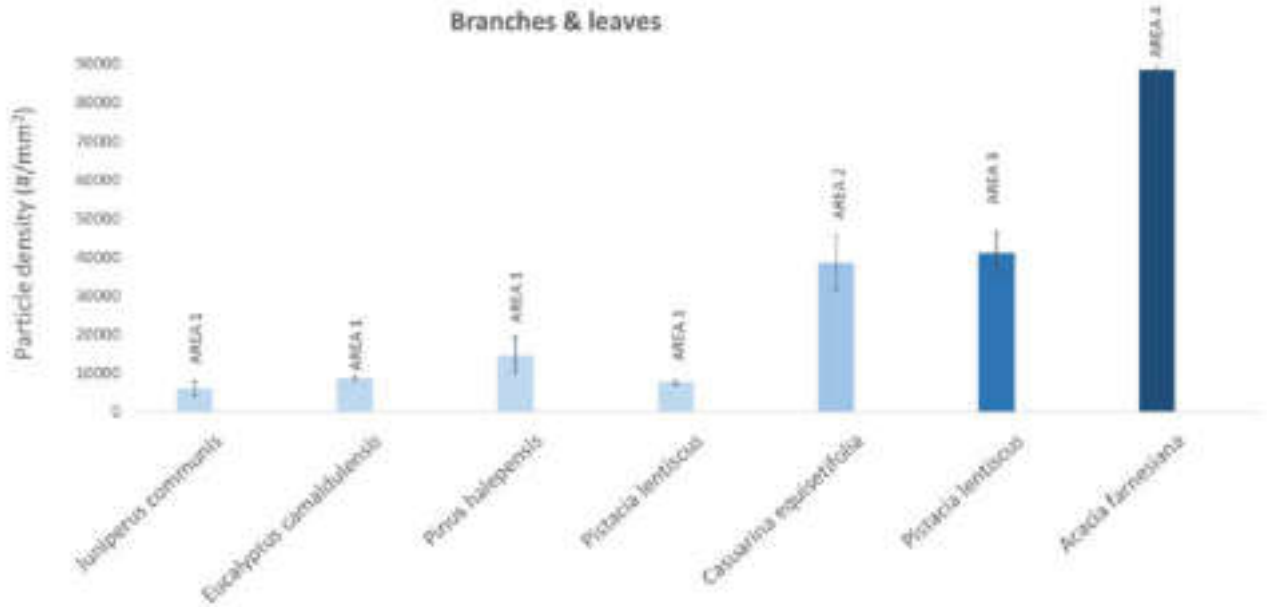

Figure 28 - Total particle density across study areas for branches and leaves. Samples of different species in different areas are presented.

Comparing litter with branches & leaves, we generally see that the combustion generates a higher density of particle on branches & leaves filters (Figure 29). This is clear for Area 2 and 3, while is not always coherent for Area 1 (see *Juniperus communis* and *Pistacia lentiscus*, Figure 29).

Generally, combustion experiments of Area 1 samples result in filters with lower particle density both for litter and branches & leaves. This aspect deserves further analysis to understand why this area is characterized by a lower number of particles.

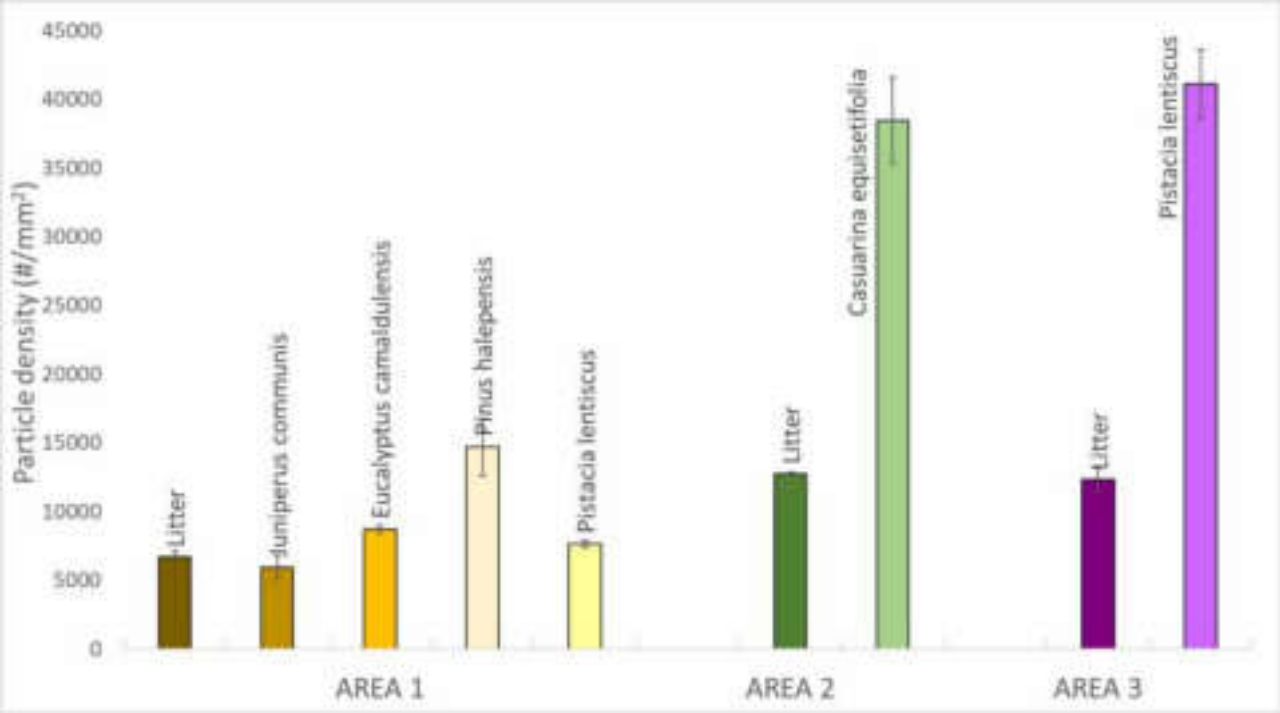

Figure 29 - Total particle density across study areas comparing litter versus branches & leaves samples.

Additionally, three PM size fractions ($PM_{10–2.5}$, $PM_{2.5–1.0}$, $PM_{1.0–0.3}$) were analysed and their distribution is reported in Figure 30. All locations have at least 92% of the particles having an aerodynamic diameter below 1.0 µm ($PM_{1.0–0.3}$), from 0.3 to 8 % belonging to the $PM_{2.5–1.0}$ fraction and less than 1 % of coarse particles ($PM_{10–2.5}$). This pattern is in accordance with the typical atmospheric PM size fraction distribution generally observed (Tittarelli *et al.*, 2008). *Casuarina equisetifolia* and *Acacia farnesiana* filters present the highest and the lowest values of $PM_{1.0–0.3}$, respectively (Figure 30). It is interesting to note that *Acacia farnesiana* show the highest values of $PM_{2.5–1.0}$. This peculiarity, combined with its highest particle density (Figure 28), deserve further analysis on plant morphology/physiology.

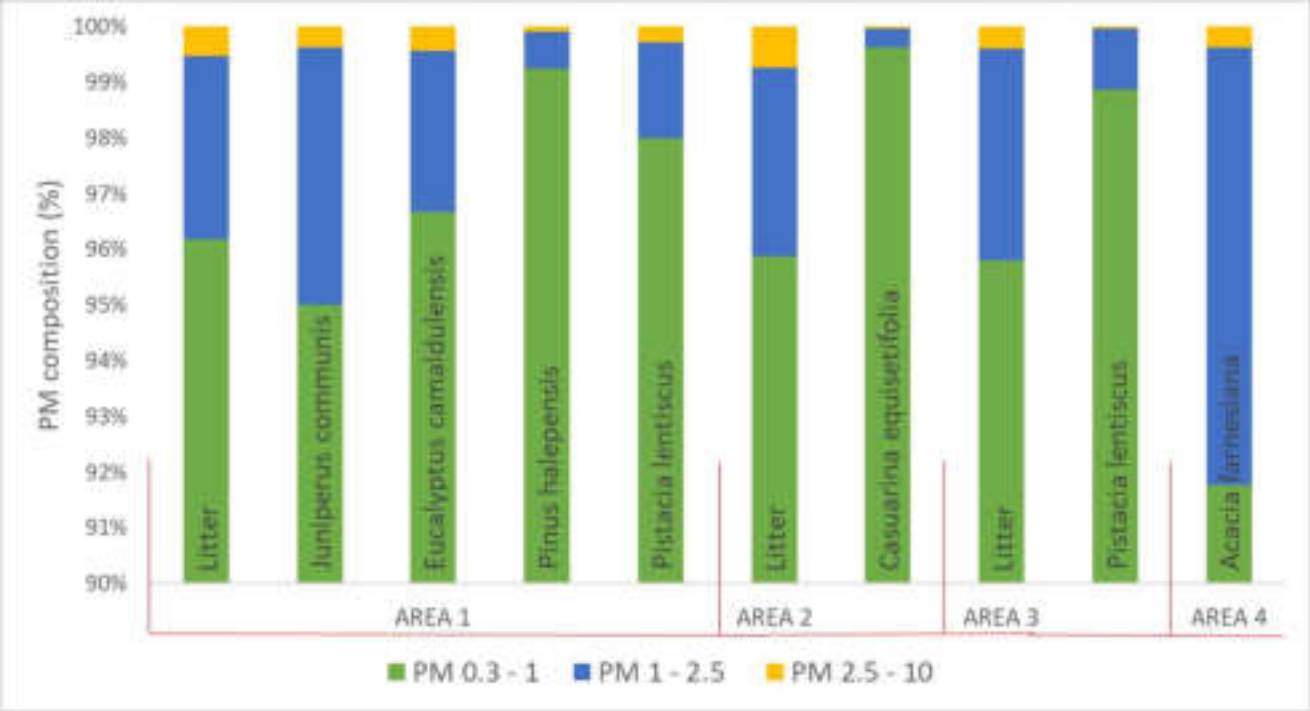

Figure 30 - PM composition per size fraction expressed as percentage. Litter versus branches & leaves samples are presented across study areas.

In conclusion, within ServForFire project, the speciation profile of emission and the analysis of PM from forest fire will contribute to the effective quantification of biomass-burning impacts on atmospheric composition and, thus, to the assessment of wildland fires impact on carbon cycle at local scale.

REFERENCES

- Nečas, D. and Klapetek, P. (2012) 'Gwyddion: An open-source software for SPM data analysis', Central European Journal of Physics, 10(1), pp. 181–188. doi: 10.2478/s11534-011-0096-2.
- Pallozzi, E. et al. (2018) 'Differences between a deciduous and a conifer tree species in gaseous and particulate emissions from biomass burning', Environmental Pollution. Elsevier Ltd, 234, pp. 457–467. doi: 10.1016/j.envpol.2017.11.080.
- Sgrigna, G. et al. (2020) 'Relationships between air particulate matter capture efficiency and leaf traits in twelve tree species from an Italian urban-industrial environment', Science of the Total Environment, 718(137310).
- Tittarelli, A. et al. (2008) 'Estimation of particle mass concentration in ambient air using a particle counter Estimation of particle mass concentration in ambient air using a particle counter', Atmospheric Environment. Elsevier Ltd, 42(November), pp. 8543–8548. doi: 10.1016/j.atmosenv.2008.07.056.

Nečas, D. and Klapetek, P. (2012) 'Gwyddion: An open-source software for SPM data analysis', *Central European Journal of Physics*, 10(1), pp. 181–188. doi: 10.2478/s11534-011-0096-2.
Pallozzi, E. *et al.* (2018) 'Differences between a deciduous and a conifer tree species in gaseous and particulate emissions from biomass burning', *Environmental Pollution*. Elsevier Ltd, 234, pp. 457–467. doi: 10.1016/j.envpol.2017.11.080.
Sgrigna, G. *et al.* (2020) 'Relationships between air particulate matter capture efficiency and leaf traits in twelve tree species from an Italian urban-industrial environment', *Science of the Total Environment*, 718(137310).
Tittarelli, A. *et al.* (2008) 'Estimation of particle mass concentration in ambient air using a particle counter Estimation of particle mass concentration in ambient air using a particle counter', *Atmospheric Environment*. Elsevier Ltd, 42(November), pp. 8543–8548. doi: 10.1016/j.atmosenv.2008.07.056.

1.6 Fire emission Estimation using Landsat TM: the case study studies of 2011 fires occurred in the Ionian coast (southern Italy)

Contribution by CNR-IMAA: Cardettini G., Aromando A., Proto M., Lasaponara R.

Fires are considered as one of the most important causes of degradation being that they induce significant alterations not only on the vegetation cover but also on fauna, soil, atmosphere thus producing high direct and indirect damages including economic ones. At a global scale, yearly 50 million hectares of forest are burnt producing a significant impact on global atmospheric pollution, being that biomass burning contributes to the global budgets of greenhouse gases, like carbon dioxide, etc. Actually, wildfires contribute to carbon emissions and human-induced climate change, a process that is likely to cause progressive aridness of parts of Europe with increased risk for wild fire and subsequent secondary disasters such as erosion, floods and landslides. At a global scale forest fires produce a remarkable amount of greenhouse gases and solid particulate matter.
Current and future challenges of wildfire contrast and governance, oriented to a comprehensive approach to limit fire incidence, can be addressed creating a system focused on social and ecological resilience and based on reliable and update information on fire occurrence and characteristics, including the assessment of fire damage with specific reference to the missions from forest fires which depend on (1) the duration and intensity of the fire, (2) the total area burnt by the fire, and (3) the type and amount of the burnt vegetation generally referred to as fuel load. In our study case, we used the fuel load mapping developed for the Basilicata region in the framework of FIRESAT project based on Landsat TM data and assessed the burnet areas using Landsat TM data acquired before and after the fire event. The assessment of the emission is based on the formula:

$$E x = F (A, B, C, E)$$

Where: - Ex emission of compound x –
A: burnt area (m2) – estimated from Landsat
B: fuel load (g dry matter m-2) – estimated from Landsat (in terms of Fuel load as developed for the Basilicata in the framework of FIRESAT project)

C: burning efficiency – estimation from, Landsat (in terms of fire severity)
E: emission factor (g g-1 dry matter burnt) for which we used CO, CH4, VOC, NOx, N2O and SOx taken from the current state of the art as available in Miranda et al. (2005).

1.7 High Resolution Seasonal Forest Fire Danger mapping for Greece and South Italy

Contribution by NCRSD: Varela V., Vlachogiannis D., Sfetsos A., Karozis S.

The purpose of this work was the calculation of the Canadian FWI system indices of the Canadian System CFFDRS (Van Wagner et al 1985) combined with a state-of-the-art seasonal meteorological forecasting model, for predictive high resolution fire danger mapping for the fire period of the year 2020, for Greece and South Italy, as a tool to design medium-term prevention planning.

More specifically, the calculation of a series of seasonal forecasted maps of meteorological fire danger, for three months of the fire season 2020, for the two areas, using the Fire Weather Index (FWI) system. To this end, three components of the FWI system have been calculated, analysed and mapped namely, the Drought Code (DC), Fire Weather Index (FWI) and Daily Severity Rating (DSR) for the referenced period. The meteorological data needed for the calculation of FWI are produced from high resolution simulations with the WRF model (v3.5.1), for a period of six (6) months, using a grid spacing of 5x5 km covering the whole Greece and South Italy. WRF-ARW model (version 3.5.1) has been suitably parameterized for high resolution production medium-term (seasonal) forecasts for the two areas.

Initial boundary conditions for the WRF model simulations, were determined by twelve-hour analyses provided by the Climate Forecast System of Environmental Prevention, at 00 and 12 UTC for the time period of interest (Saha et al., 2010)

The above referenced indices are calculated for every day of the referenced period. Then the following series of final maps were calculated for from the derived daily maps for the two areas of interest.

- Weekly maps of number of days in very high and extreme FWI class (FWI > 50 for Greece and FWI > 38 for Italy)
- Monthly maps of DC mean values
- Monthly Severity Rating (MSR) maps

The DSR is a transformation of the daily FWI value, calculated as follows (Van Vagner et al,1985):

DSR = 0.0272FWI^ 1.77

Higher FWI values are emphasized through the power relation. The DSR can be accumulated over time as the cumulative DSR, or it may be averaged over a month as the MSR.

The context of the individual FWI system components which were selected in this study is described briefly below:

- The Drought Code (DC) is a numeric rating of the average moisture content of deep, compact organic layers. This code is a useful indicator of seasonal drought effects on forest fuels and the amount of smouldering in deep duff layers and large logs.
- FWI represents the potential fireline intensity and it is a good indicator of general fire danger (Viegas et al 1999).
- The Daily Severity Rating (DSR) is a numeric rating of the difficulty of controlling fires. It is based on the Fire Weather Index but more accurately reflects the fire suppression

expected efforts (Van Wagner et al, 1985). MSR is the mean value of the DSR during a month.

The resulting maps are presented below:

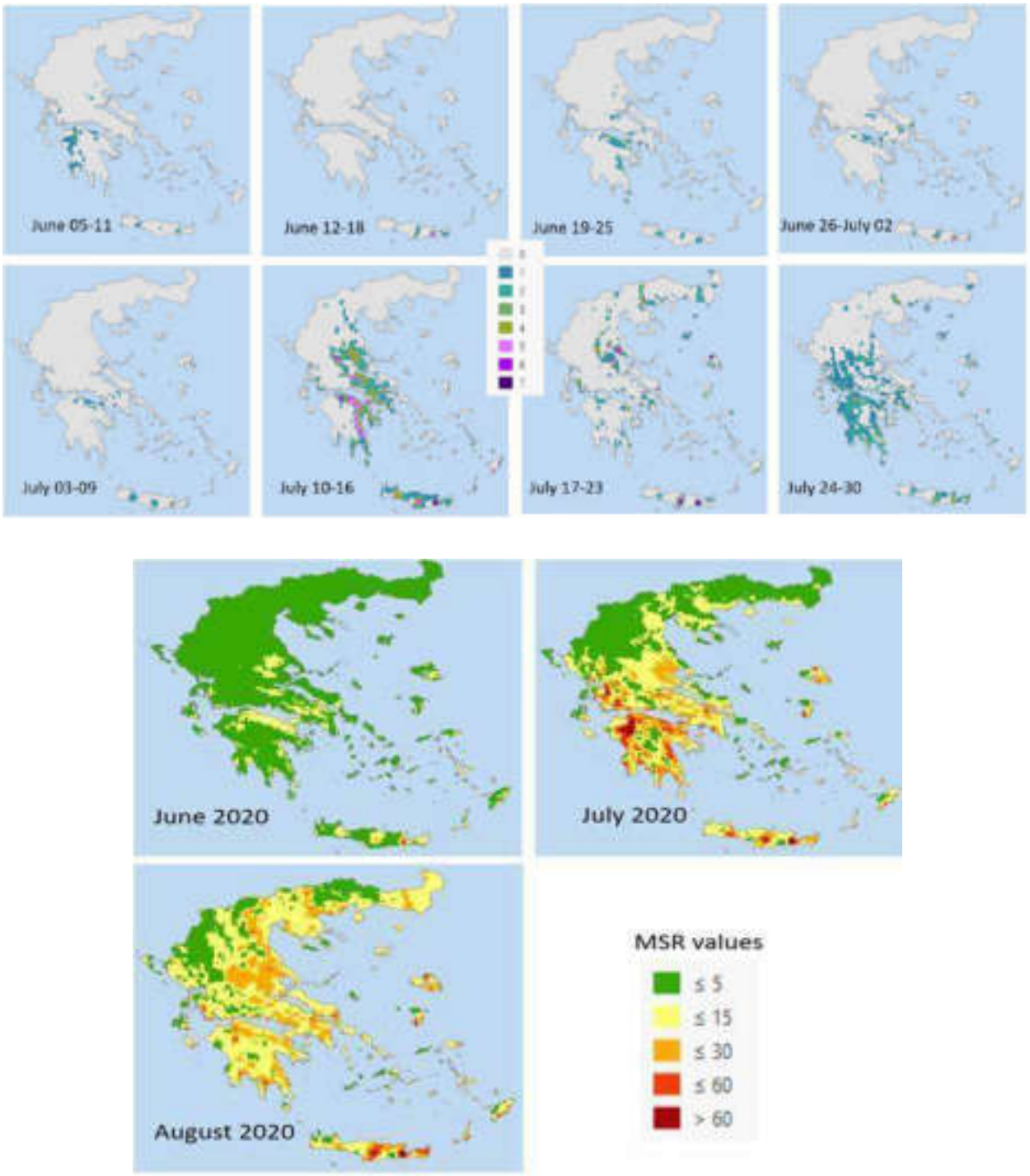

Figure 32 - Monthly Severity Rating Maps for June, July and August 2020, for Greece

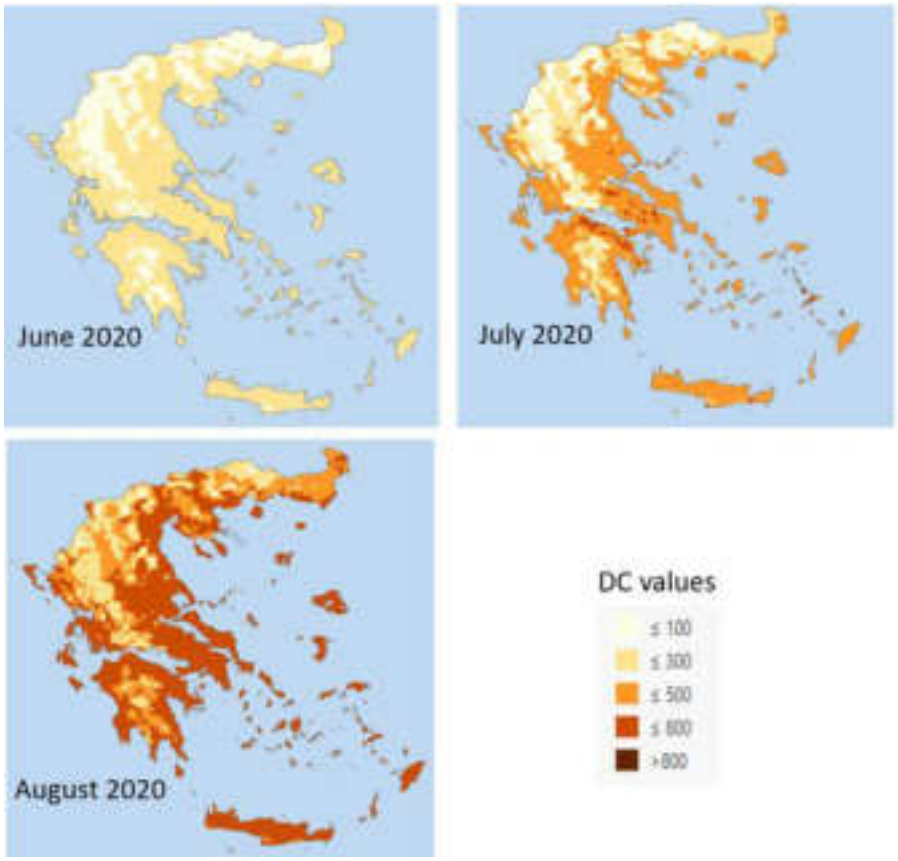

Figure 33 - Monthly Mean Drought Code Maps for June, July and August 2020, for Greece.

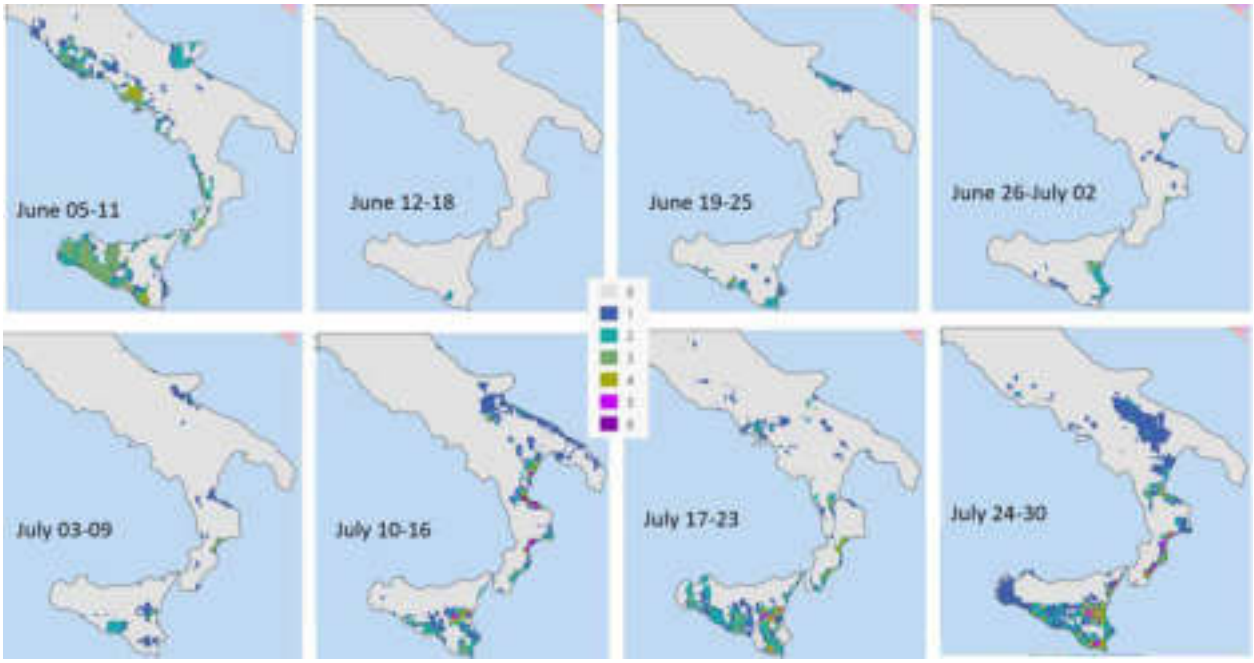

Figure 34 - Weekly maps of the number of days with very high and extreme FWI class (FWI>50) for June – July 2020, for South Italy.

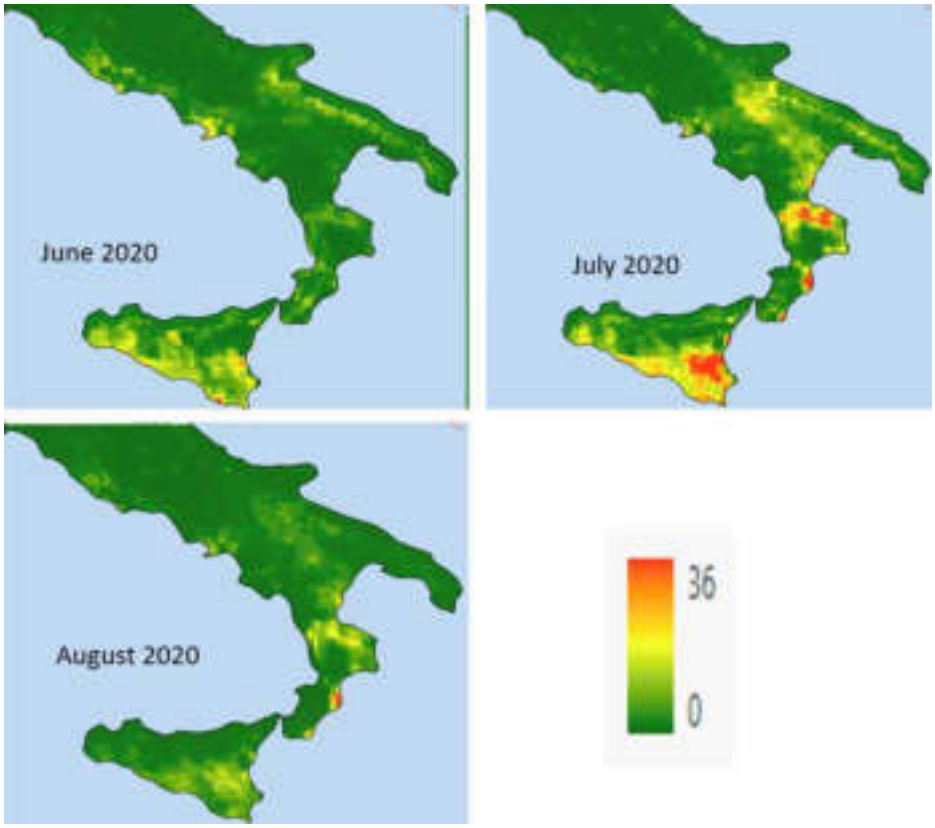

Figure 35 - Monthly Severity Rating Maps for June, July and August 2020 for South Italy.

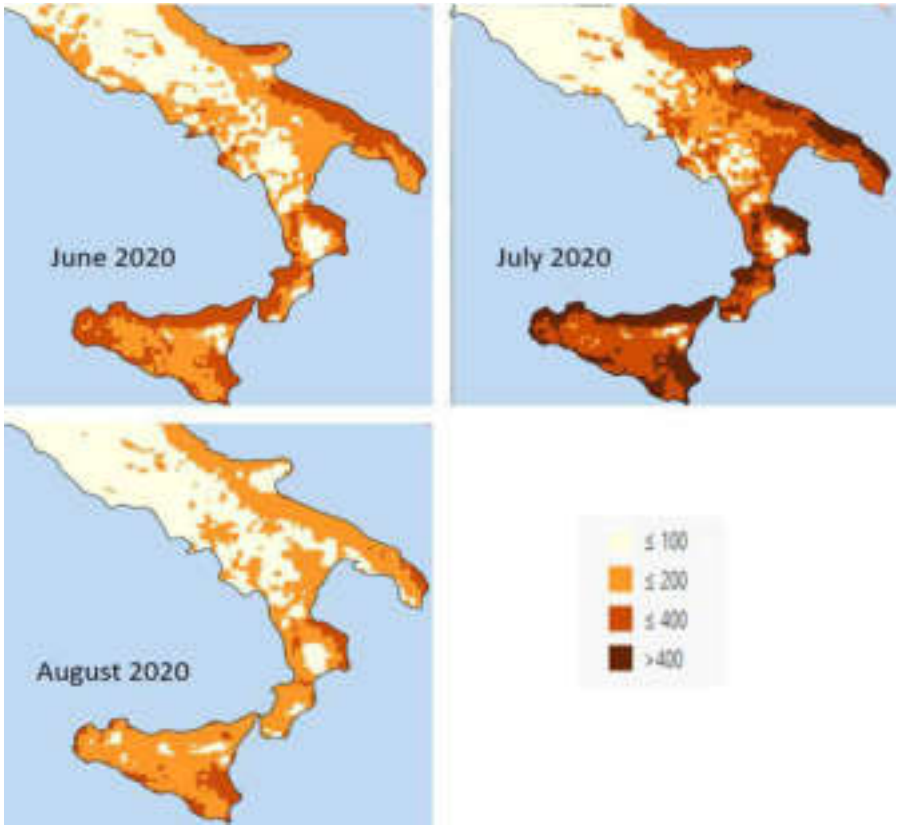

Figure 36 - Monthly Mean Drought Code Maps for June, July and August 2020 for South Italy.

REFERENCES

- Van Wagner, C.E. Development and Structure of the Canadian Forest Fire Weather Index System; Forestry Technical Report; Canadian Forestry Service: Ottawa, ON, Canada, 1987; Volume 35, 35p
- Van Wagner, C.E.; Pickett, T.L. Equations and FORTRAN program for the Canadian forest fire weather indexsystem. Available online: https://cfs.nrcan.gc.ca/publications?id=19973 (accessed on 15 June 2020)
- Viegas, D.X.; Biovio, G.; Ferreira, A.; Nosenzo, A.; Sol, B. Comparative study of various methods of fire danger evaluation in southern Europe. Int. J. Wildland Fire 1999, 10, 235–246.
- Saha, S., and Coauthors, 2010: The NCEP Climate Forecast System Reanalysis. Bull. Amer. Meteor. Soc., 91, 1015–1057.

1.8 Climate attribution study of the forest fires in Portugal 2017

Contribution by KNMI: Krikken F., van Oldenborgh G.J., van Velthoven P.

Climate attribution studies for recent extreme forest fires are the main activities carried out by KNMI, apart from seasonal forecasts of fire weather.
The forest fires in Portugal 2017 were selected as a case study because of the severity of the fires and the impact it had on society, specifically the large number of casualties.
We follow the same method previously applied to the climate attribution of the forest fires in Sweden 2018 (Krikken et al., in review). We use Canadian fire weather index (FWI) to quantify the fire weather risk. We construct the FWI using ERA5 reanalysis data and two climate models (EC-Earth and CESM). The former is used to get an observational estimate, while the latter is used to get an estimate of past, present and future fire weather risk.

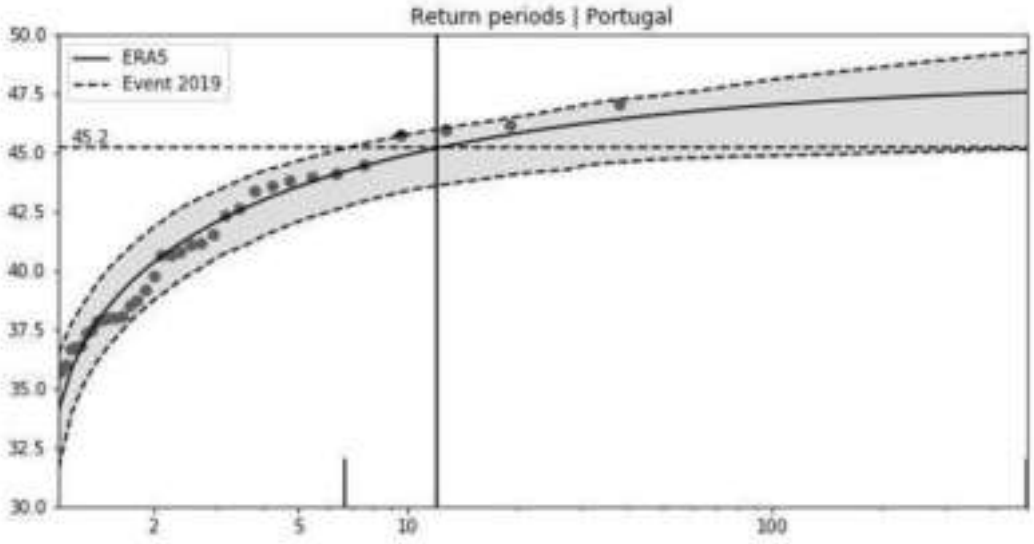

Figure 37 - Return times of the 2017 forest fire event, based on ERA5 reanalysis data

Figure 37 shows the return time of the 2017 forest fire event, defined as the maximum FWI during the fire season, averaged over Portugal, with a 7-day rolling mean applied. The return time of ~11 years indicate that based on only the fire weather, it was indeed a rare event but not unprecedented over the last 40 years.

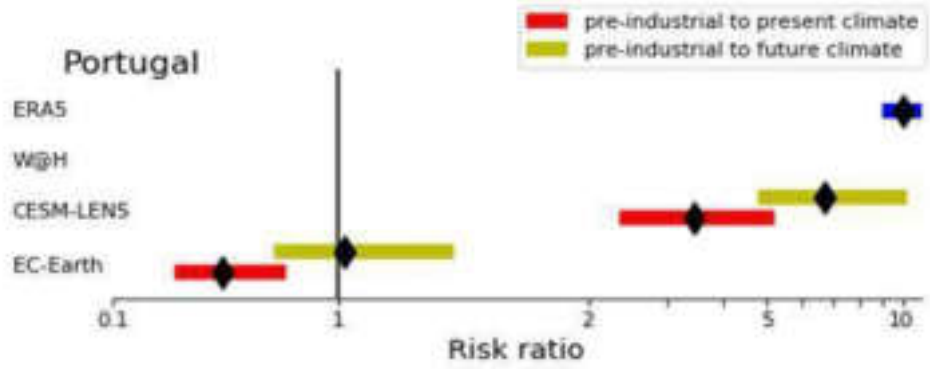

Figure 38 - Risk ratios of the Portugal 2017 forest fires, for ERA5 (reanalysis) and CESM and EC-Earth (climate models). The risk ratios are given relative to pre-industrial climate.

Figure 38 illustrates the risk ratios, i.e. how much more or less likely such an event has become relative to pre-industrial climate. We can see that based on ERA5, the event has become ~10 times more likely. Both climate models show distinct different responses, where CESM gives a large increased risk for such event both for current and future climate. EC-Earth however shows decreased risk for such an event for the present climate and the same risk for future climate.

Our aim is to continue this analysis with more reanalysis products and climate models, and to better understand the distinct different behaviour between the climate models used, in order to give accurate projections of future fire weather risk in the Mediterranean region.

REFERENCES

- Krikken, F., Lehner, F., Haustein, K., Drobyshev, I., and van Oldenborgh, G. J.: Attribution of the role of climate change in the forest fires in Sweden 2018, Nat. Hazards Earth Syst. Sci. Discuss., https://doi.org/10.5194/nhess-2019-206, in review, 2019.

1.9 The use of Random Forest classifier for the mapping of burnt areas based on satellite data Sar (Sentinel1) and optical data (Sentinel 2). The case study: fire in the South of Portugal in 2018"

Contribution by CNR-IMAA: Fattore C., Lasaponara R.

In the recent years, forest fires in Portugal have become a serious environmental problem. According to the 2017 annual report issued by EFFIS (European Forest Fire Information System), the number of fires occurred was about 21002 for a burnt area of about 540630 hectares; in 2018 the burnt areas decreased, but 37436 hectares were affected.
The study area is located in Southern Portugal, particularly in the Algarve region. The event, which took place in August 2018, damaged the city of Monchique and burned about 27,000 hectares. The satellite data used for mapping the burnt areas are the Optical images and the SAR images (respectively Sentinel 2 and Sentinel 1 of the ESA Copernicus program), which have different resolutions, to better understand how the two sensors return different information based on data processing. The Sentinel-2 used has a resolution of 10 m while the Sentinel-1 has a resolution of 5 m. The choice to use such high resolutions is due to the large size of the event to be investigated, in order to better detect the burn severity. The identification and mapping of the surfaces affected by the fire is based on the recognition of the spectral response of the burnt vegetation, i.e. different from the response of the unburned surface. The identification and mapping of the areas affected by the fire are based on the recognition of the spectral response of the burnt vegetation, i.e. different from the response of the unburnt surface. In this case we used spectral vegetation indices such as the NDVI (Normalized Difference Vegetation Index) and the NBR (Normalized Burn Ratio). The first was selected to estimate the moisture level in the vegetation, as the fire causes a significant decrease in the humidity level of the plants and the soil. The second index, however, is designed to highlight burnt areas and estimate the severity of the fire. The formula is similar to NDVI, except that it uses near infrared (NIR) and shortwave (SWIR) wavelengths.

A comparison was made between the limit values of the normalised combustion ratio (dNBR) and the normalised differential vegetation index (dNDVI) (from pre- and post-fire images). However, dNBR could present problems in areas with low pre-fire vegetation cover, where the absolute variation between pre-fire and post-fire NBR is not significant. For this reason, we have applied an additional spectral index such as RBR (Relativized Burn Ratio), which allow us to isolate the burned area from the unburned context (Fig. 27). Spectral indices provide information on risk assessment, severity of fire and burns, characterizing the extent of damage but they are not sufficient for discriminating burned area, so it was necessary to create a supervised classification, through the application of a special classifier such as the to the Random Forest.
The random forest classifier consists of a combination of tree classifiers where each classifier is generated using a random vector sampled independently from the input vector, and each tree casts a unit vote for the most popular class to classify an input vector (Breiman, 1999).
This procedure resulted in better classification accuracy.

It is important to carefully choose the attributes to be provided to our classifier because as they must be as meaningful as possible. In this case, our characteristics are determined by the results obtained by mapping the burned area using the spectral index RBR (Relativized Burn Ratio). The different levels of fire severity produced were also compared with the levels catalogued by the

United States Geological Survey (USGS), which proposed a classification table to evaluate the severity of the fire.
The next objective is to estimate the damage after the fire in terms of burnt vegetation, damaged soil, and carbon monoxide emissions after an accurate definition of the degree of burn.

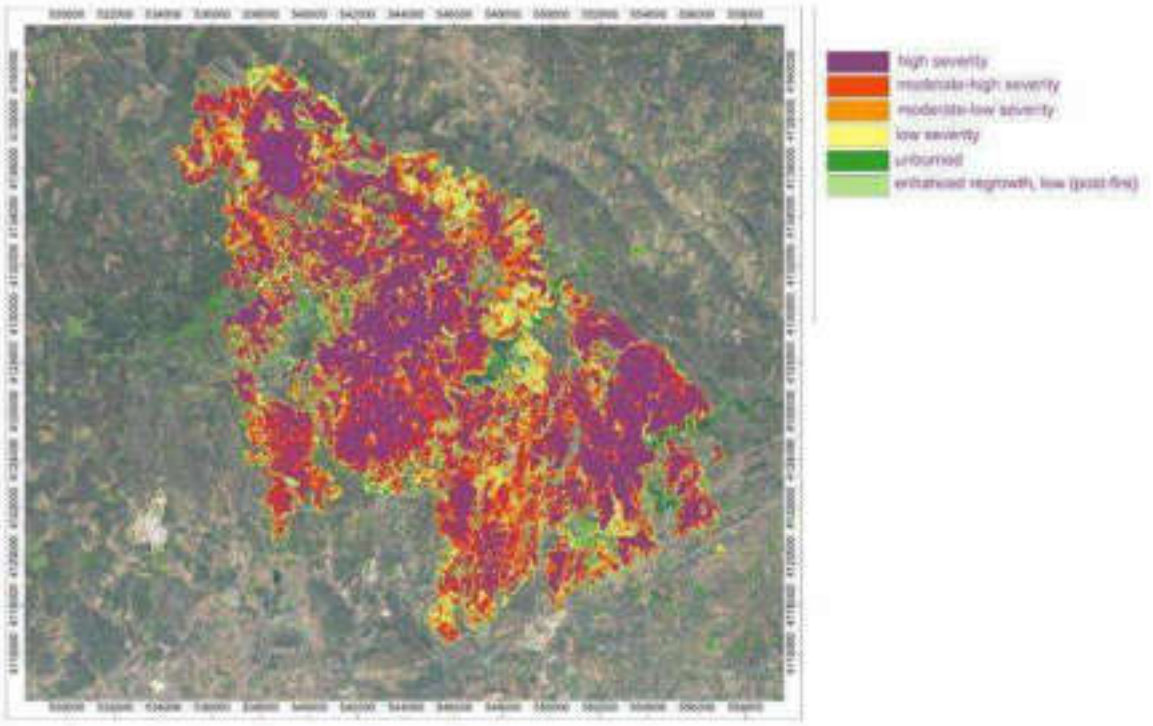

Figure 39 - Sentinel-2 RBR (Relativized Burn Ratio) index on the area affected by the fire. The legend clearly shows the most damaged areas thanks to the discrimination of fire severity.

2. Fire risk estimation: post-fire phase

1. 2.1 Post-fire phase for the area of eastern Attika

Contribution by NCSRD: Varela V.

The fire risk estimation of the post-fire phase for the area of eastern Attika is based on the simulation of fire behaviour of the fire in Mati. More particularly, G-FMIS fire simulator, which is based on BEHAVE/Rothermel's equations, was used for the calculation of fireline intensity map of the area of interest, based on the weather conditions during the fire. Fireline intensity parameter is the rate of energy or heat release per unit time per unit length of fire front (kW/m).

Figure 40 - Simulated fire propagation of Mate Fire, for the first three hours.

The overlay of the final burned area on the fireline intensity map (Fig. 40-41), depicts the fire line intensity conditions for every point within the burned area and is a good indicator of fire severity and expected post-fire effects for the particular fire.

Figure 41 - Calculated map of Fireline intensity in kW/m for the weather conditions of the fire in Mati.

2.2 POST FIRE RISK ASSESSMENT: MODELING POTENTIAL IMPACT OF FIRE ON HYDROLOGY AND SEDIMENT TRANSPORT: The Celone River Case Study

Contribution by CNR-IRSA and BRGM: Anna Maria De Girolamo (CNR-IRSA), Antonio Lo Porto (CNR-IRSA) Rosalie Vandromme (BRGM) Olivier Cerdan (BRGM)

2.2.1 The Celone River Case Study

Fire may have a severe impact on soil and water as fire-related contaminants are delivered with suspended sediment to the river and may lead to a depletion of water quality with consequences for aquatic ecosystems precluding the achievement of the Water Framework Directive objectives.

The general aim of this study is to define a procedure to assess the impact of fire on hydrology, soil losses, and sediment transport to a river network. Specific objectives are to: (i) assess the adequacy of the SWAT model to predict post-fire impacts at the basin and subbasins scale in order to be used as a post-fire management tool, and (ii) estimate potential changes in hydrological regime and soil erosion rates. The study focuses on a high temporal and spatial scale for a management perspective.

The study area, the Celone River Basin (Puglia, Italy), is classified at a high risk of fire due to weather conditions and ignition sources (deciduous and mixed forests). For the future, due to climate change, it is expected an increase in the occurrence of droughts and a reduction of streamflow (De Girolamo et al., 2020), therefore, both short and long-term post-fire contamination risks could also increase.

In this work, the impact of fire on hydrology and sediment transport was estimated by using the Soil and Water Assessment Tool, SWAT2005 version with Arcgis interface (Arnold et al., 1998) (De Girolamo et al., 2020). The model was used to estimate streamflow and sediment load for the current land use (baseline) and for the fire scenarios. The following fire scenarios were simulated:

- Scenario Fr1: high-severity fire.
- Scenario Fr2: moderate-severity fire.
- Scenario Fr3: low-severity fire.

It was assumed that in 2010 fire burned the forest areas in three selected subbasins (Sub. 28, 29, 44 in Figure 2) and that burnt areas were left for natural regeneration in 2011.

Fire impact was simulated considering two main factors, the increase of runoff due to soil water repellency in burnt areas and the reduction of soil protection due to the damage of vegetation cover. The increase of runoff was estimated by modifying parameters such as the Manning's roughness coefficient (OV_N), the initial SCS runoff Curve Number for soil moisture condition II (CNII), and saturated hydraulic conductivity (Sol_K). The reduction of soil protection was assessed modifying the USLE C factor for water erosion of soil, the USLE equation support practice factor USLE_P, the USLE erodibility factor USLE_K, and the leaf area index (LAI). The modified values are reported in Table 1.

Table 1. SWAT parameters used in the baseline simulation and in the fire scenarios simulations.

	Baseline	High severity	Moderate severity	Low severity
Ov_n	0.4	0.2	0.25	0.3
USLE_P	0.8	1	1	1

USLE_C	0.002	0.2	0.15	0.1
CNII	70	94	87	80
Soil K (mmh^{-1})	0.9-2.4	-15%	-10%	-5%
LAI	4.8	0.9	1.5	3.5
USLE_K*	0.13-0.15	+15%	+10	+5%

*(ton acre h)/ (acre ft ton inch)

2.2.2 Modelling hydrology and sediment yield for the current conditions (baseline)

The performance of the model simulation was evaluated by using the Nash and Sutcliffe efficiency (NSE) and correlation coefficient (R2). For hydrology, the model was calibrated comparing measured and simulated streamflow at the daily time scale at the outlet over the period 1996, the NSE was 0.65, the R^2 value was 0.87. In the validation period (2010-2011), NSE was 0.67, and R2 was 0.87. For the sediment load, the model was calibrated at the outlet on the monthly time scale for the period 2010-2011 (NSE= 0.74, R^2 = 0.89).

Mean annual water yield (TWY) estimated from 1990 to 2011 ranged from 177mm y^{-1} to 364mm y^{-1}. Wide inter-annual variability in TWY was found in the study period due to the large difference in rainfall amount from one year to another. Spatial variability within the basin was also recorded, it was mainly due to geological and lithological factors. Figure 1 shows the mean annual TWY at the subbasin scale.

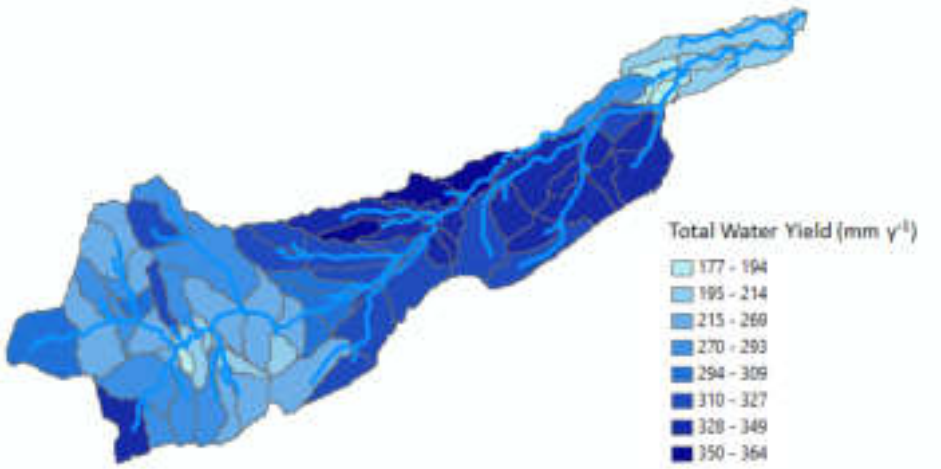

Figure 42 - Average annual value of total water yield (mm y-1) at the subbasin scale estimated from 1990 to 2011.

At the outlet of the basin, the mean annual specific sediment load (SSL) estimated over the period 1990 to 2011 was 5.27 t ha^{-1} y^{-1}, ranging from 1 t ha^{-1} y^{-1} to 11 t ha^{-1} y^{-1}. Most of the annual load was delivered during the wet season, from December to March. Land use and slope were the main factors influencing soil erosion.

At the subbasin scale, the areas characterized by steep slope and pasture or bare soil showed the highest values of soil losses. Among agricultural crops, durum wheat production in hilly areas, where up-and-down tillage was generally adopted, showed high values of soil losses. Figure 2 shows the average annual sediment yield at the subbasin scale.

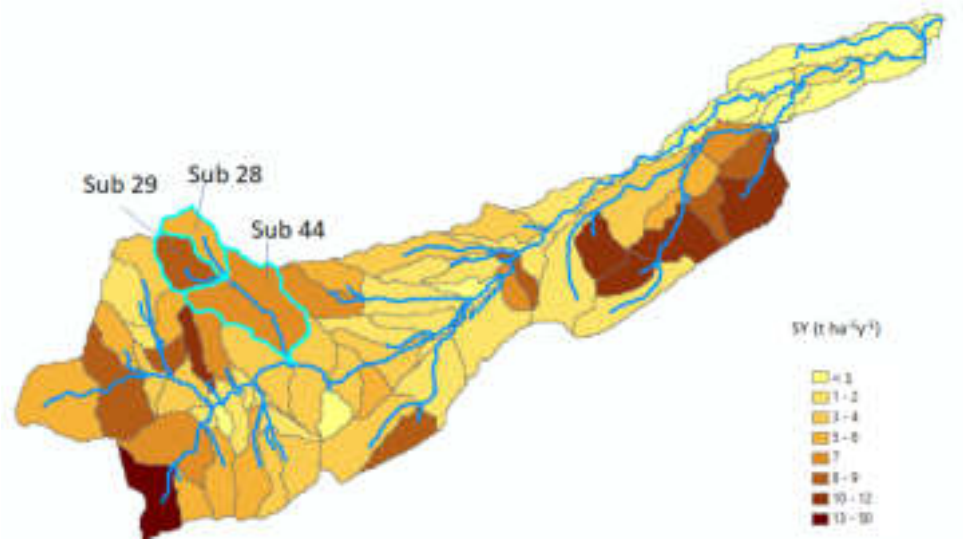

Figure 43 - Average annual value of specific sediment yield (t ha-1 y-1) at the subbasin scale estimated from 1990 to 2011

2.2.3 Modelling hydrology and sediment yield under fire scenarios

Fire scenarios were simulated in three subbasins where forest (deciduous, evergreen, and mixed forest) was 53%, 19%, and 31% of the Subbasin 28, 29, and 44, respectively (Figure 2). The potential impact of the fire was analysed at the sub-basin level. The comparison of the baseline and scenario Fr1 and scenario Fr3 was carried out for two years, 2010 and 2011, since as reported in the literature, the highest hydrological and erosive events occur beyond the first year. Table 2 summarizes changes in runoff and SSY at the subbasin scale simulated by the SWAT model for both scenarios. In 2010, for the scenario Fr1, TWY increased from 3 to 12% compared to the baseline depending on the percentage of the area of the subbasin occupied by forest. A lower increase of TWY was simulated in the low impact scenario Fr3 (from 1% to 3%).

Sediment yield increased in the analysed basins ranging from 24 t ha-1 y-1 to 54 t ha-1 y-1 under scenario Fr1 and from 14.60 t ha-1 y-1 to 21.90 t ha-1 y-1 under scenario Fr3. In 2011, the increase of TWY and SSY was reduced compared to the first year of fire occurrence. However, soil losses were higher than the baseline, especially for the Subbasin 28 and 44, where severe soil erosion was simulated.

Table 2. Total water yield (TWY, mm) and specific sediment yield (SSY, t ha^{-1} y^{-1}) simulated by the SWAT model in three subbasins for the current condition (baseline) and for fire scenarios (Fr1: high-severity fire; Fr3: low-severity fire).

Year	Sub	Total Water Yield (mm)			Specific Sediment Yield (tha^{-1} y^{-1})		
		Baseline	Scen. Fr1	Scen. Fr3	Baseline	Scen. Fr1	Scen. Fr3
2010	28	449	505	463	3.03	54.25	14.60
	29	502	519	509	7.92	24.02	12.96
	44	472	497	482	9.63	47.50	21.90

2011	28	281	291	289	1.68	29.66	13.38
	29	306	305	306	3.54	11.66	7.56
	44	303	303	304	6.23	24.57	15.76

2.2.4 Perspectives

Based on the temporally-detailed results obtained using the SWAT model, using a subbasins approach, a spatially-detailed analysis will be performed using the WATERSED model (Landemaine, 2016; Baartman et al., In press). Thus, different scenarios will be modelled in order to quantify the effect of the spatial distribution of forests in the landscape under different reforestation and fire scenarios. These modelling results will highlight strategic areas of the landscape that should (or should not) be reforested in order to limit runoff, erosion and sediment transfers to the river network, taking into account reforestation strategies and the effects of subsequent forest fires.

REFERENCES

- Baartman J.E.M., Nunes J.P., Masselink R., Darboux F., Bielders C., Degre A., Cantreul V., Cerdan O., Grangeon T., Fiener P., Wilken F., Schindewolf M., Wainwright J. What do models tell us about water and sediment connectivity? Geomorphology, In press.

- De Girolamo A.M., Lo Porto A., 2020. Potential flow regime alterations under climate change in an intermittent river system. EGU2020-22542. https://doi.org/10.5194/egusphere-egu2020-22542

- Landemaine, 2016. Érosion des sols et transferts sédimentaires sur les bassins versants de l'Ouest du Bassin de Paris: analyse, quantification et modélisation à l'échelle pluriannuelle. PhD Thesis. Rouen University.

2.3 On the impacts that fire on soil and hydrogeological risk: the case study of Basilicata Region

Contribution by CNR: Lasaponara R. (IMAA), Danese M. (IBAM)

Managers need to be aware of the impacts that fire can have on soil systems, and how these impacts can lead to undesired changes in site productivity, sustainability, biological diversity, and watershed hydrologic response. For this reason, providing reliable and qualified information on the impact of fire on vegetation and soil and related changes is crucial to maximize post fire risk prevention and related potential damage.
In this paper, we present outputs from research activities we conducted in the framework of the FIRESAT project (funded by the Office of Civil Protection of the Department of Infrastructure of the Basilicata Region) in the context of burn severity mapping addressed to the estimation of post fire damage mainly for the (i) assessment of the impact of fire on soil and hydrological risk and (ii) to support the definition of mitigation strategy.
At local scale, managers need to be aware of the impacts that fire can have on soil systems, and how these impacts can lead to undesired changes in site productivity, sustainability, biological

diversity, and watershed hydrologic response. For this reason, the availability of reliable and timely information on fire affected areas and burn severity (and expected changes) is crucial to mitigate post fire damage and optimize strategies related to post fire damage management.

The full exploitation of data provided by the diverse satellite sensors (MODIS, TM, ASTER; Sentinel 1 and 2), ancillary information and data base, with specific reference to the landslides catalogues, are integrated with all the available information (in digital and non-digital format) within a GIS environment for the elaboration, integration and publication (via a webgis. Statistical analysis on the co-occurrence of fires and landslides enable us to assess the impact of fire events on the landslide susceptibility and to provide useful information for improving landslides risk estimation and mitigation strategies. As an example, Figure 44 and 45 show the co-occurrence of fires and landslides as assessed for the 2011 and 2012 in the Basilicata Region.

Figure 44 - Co-occurrence of fires and landslides (orange dots in the figure) as assessed for the 2011 events in the Basilicata Region.

Figure 45 - Co-occurrence of fires and landslides (red dots in the figure) as assessed for the 2012 events in the Basilicata Region

2.4 On the use of Sentinel-2 for mapping burnt areas through unsupervised classification ISODATA. The European cases: Portugal, Germany and Greece.

Contribution by CNR-IMAA: Fattore C., Lasaponara R.

This study deals with the mapping of burnt areas using Sentinel-2 (S2) optical sensors which detect changes in surface reflectance.
In addition, the use of multi-level ISODATA classifications performed at both pixel and feature level allowed a significantly decreased number of false alarms and improved mapping of burnt areas.
The feature extraction of the S2 was performed using statistical analysis (LISA) and their combinations obtained through the unsupervised joint-classification. As part of our investigations, we focused on a few case studies: The first fire occurred on 3 August 2018, which affected about 27000 hectares of Mediterranean scrub and forests in southern Portugal, in the Algarve region around the city of Monchique; the second fire occurred on 3 June 2019 and it involved an area of 655 hectares of agricultural area and forests, in the north-eastern part of Germany, close to Luckenwalde which is part of the Brandeburg district; the third fire occurred on 12 August 2019 and affected about 2350 hectares of forests, heterogeneous agricultural areas and arable land near the village of Makrimalli on the island of Evia, Greece.
The estimation of the burnt areas was performed from optical satellite data, using mainly spectral indices based on band combinations (e.g. Normalized Difference Vegetation Index (NDVI), Burn Area Index (BAI), see Lasaponara et al. 2013), adopted as proxies of vegetation status. Spectral combinations of different bands are widely used for discrimination of burnt areas, as they generally tend to emphasize the spectral changes caused by fire on vegetation. One of the most

effective indices is the normalized combustion ratio (NBR) calculated as the normalized difference between NIR and SWIR bands (see formula 1):

$$NBR = (NIR - SWIR) / (NIR + SWIR) \quad (1)$$

NBR is particularly sensitive to changes in the amount of live green vegetation, moisture content and some soil conditions that may develop after the fire such as the presence of ash, reduced transpiration of vegetation and increased surface temperature due to loss of vegetation cover. All these effects increase reflectance in the mid-infrared and reduce surface reflectance in the near-infrared. The difference between pre-fire and post-fire NBR from the images is used to calculate the Delta NBR (dNBR or ΔNBR), which can be used to estimate the burn severity, i.e. it describes how the intensity of the fire affects the ecosystem functioning in the area that was burned. The effects observed often change both within the area and between different ecosystems. Burn severity can also be described as the degree to which an area has been altered by fire. A high dNBR value indicates greater damage, while areas with negative dNBR values may indicate regrowth after a fire. The formula used to calculate dNBR is:

$$dNBR = NBR_{pre\text{-}fire} - NBR_{post\text{-}fire} \quad (2)$$

The classifications were made using 3 and 5 classes adopted for the following reasons: i) five classes were used because in the USGS and EFFIS system there are five classes related to the different levels of burning and the three classes were used to discriminate the level of fire severity only on the burnt area through the perimeters provided by EFFIS EMSR. Therefore, the rationale behind this decision is the fact if we need to identify and map the pixels affected by the fire, all the different potential levels of burnt areas must be considered.
To improve the mapping of the burnt area, the spectral indices of fire calculated on S2 were first classified separately, and then, the indices that worked best were reclassified to both (i) pixel level and (ii) feature level using the Local Indicators of Spatial Association (LISA) analysis, Moran's I for the extraction of relevant features of S2 that were merged through ISODATA classification.
The selection of the unsupervised ISODATA classification was made to limit human intervention in setting the algorithm parameters as much as possible. The importance of applying the unsupervised classification is this: (i) it is an automatic process, requiring only a minimum amount of initial input compared to controlled data processing; (ii) classes do not need to be defined a priori; (iii) classes of unknown characteristics can be discovered. A number of unsupervised classification algorithms are commonly used in remote sensing, including (i) K-means clustering, and (ii) ISODATA which are quite similar. In both, the user only needs to indicate (i) the number of default classes (clusters) and (ii) the number of iterations to be performed. In the present case, the ISODATA method has been chosen because satisfying results are expected in different environments and applications.

Moreover, the results obtained from the ISODATA classification of S2 performed at pixel level (at a spatial resolution of 20 m) are well suited to the Pleiades-based maps available free of charge on the Copernicus emergency site (https://emergency.copernicus.eu/mapping/list-of-activations-rapid) obtained from PléiadeS1A/B (at a spatial resolution of 2 m). This clearly shows that the approach proposed here has allowed a rapid and accurate identification and mapping of burnt areas obtained by using the ISODATA classification of S2. Finally, the comparison of our S2

results with the EFFIS Copernicus fire severity map, obtained from VIIRIS data at a spatial resolution of 300m, clearly shows that the proposed methodology can be adopted and improved to classify the fire severity in the EFFIS system using Copernicus data.

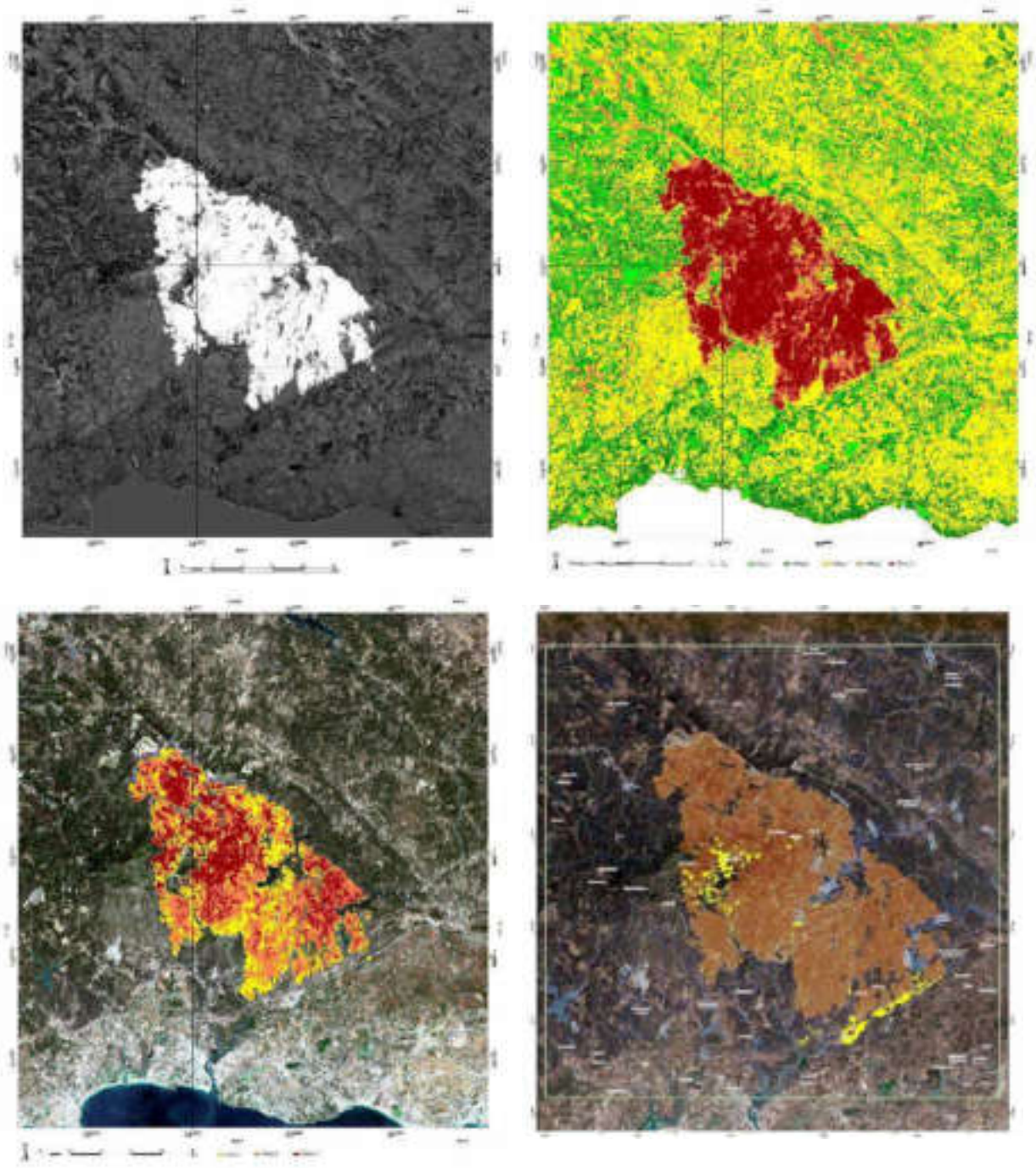

Figure 46 - On the top: dNBR index of Monchique, Portugal and ISODATA and LISA classification 5 classes. On the bottom: ISODATA and LISA classification 3 classes and Very High-Resolution satellite Pleiades Copernicus emergency Site (https://emergency.copernicus.eu/mapping/listofcomponents/EMSR303)

e) dNBR index of

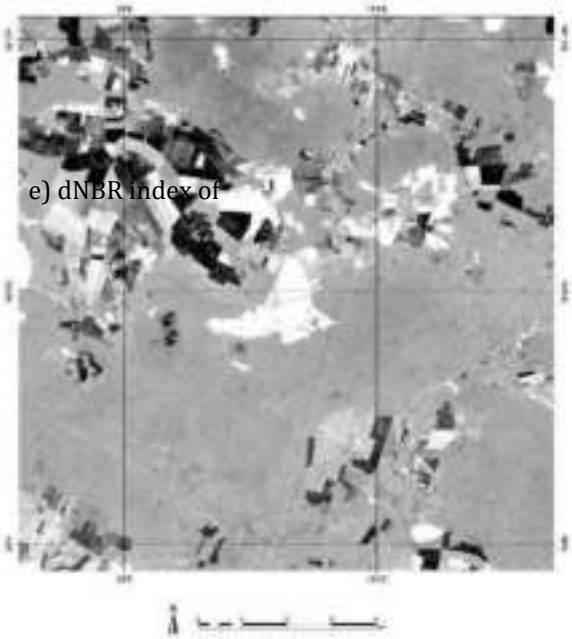

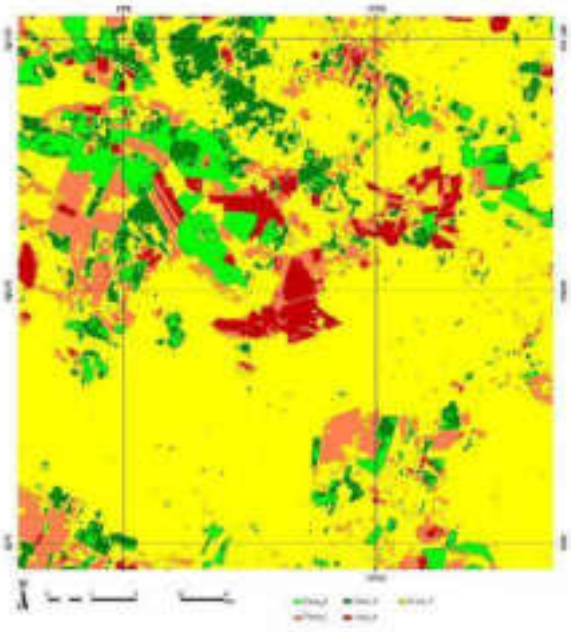

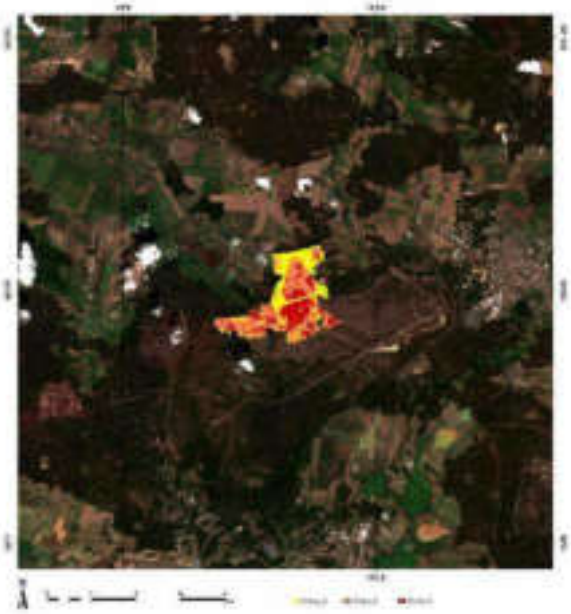

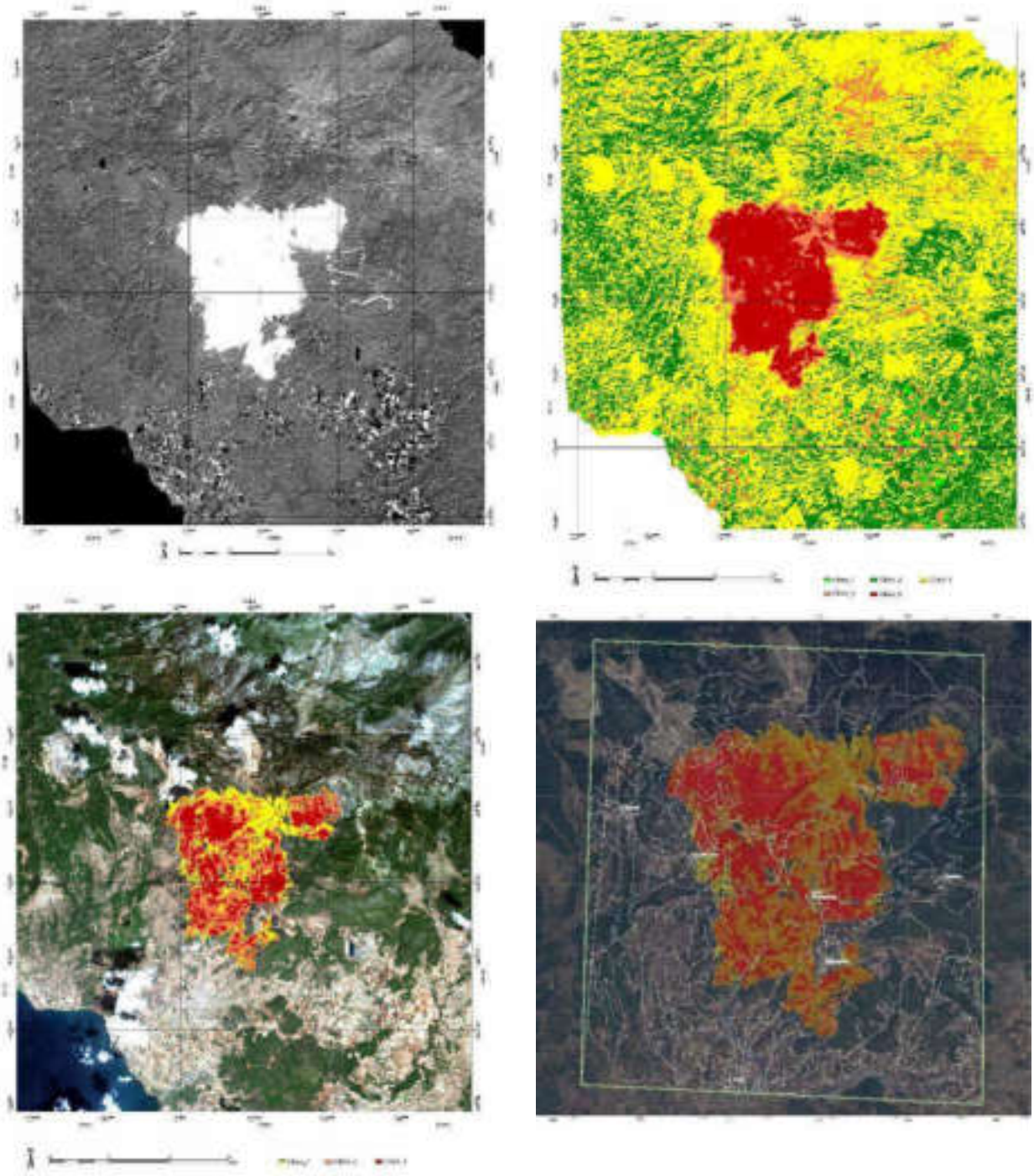

Figure 48 - On the top: dNBR index of Makrimalli, Greece and ISODATA and LISA classification 5 classes. On the bottom: ISODATA and LISA classification 3 classes and Very High-Resolution satellite Pleiades Copernicus emergency Site (https://emergency.copernicus.eu/mapping/listofcomponents/EMSR380)

3. Publications

- Carmen Fattore, Rosa Lasaponara. Analysis, interpretation and discussion on mismatch of Fire severity mapping from UAV, Sentinel -2 and EFFIS: case studies in the Basilicata Region. 12th EARSEL Forest Fires SIG Workshop “Remote sensing of forest fire data, science and operational applications” Conference, 3-5 October 2019 - Rome, ITALY
- Di Giuseppe, E., Pasqui, M., Magno, R., & Quaresima, S. (2019). A Counting Process Approach for Trend Assessment of Drought Condition. Hydrology, 6(4), 84.
- Emanuele Pallozzi, Ilaria Lusini, Lucia Cherubini, Ramilla. Hajiaghayeva, Paolo Ciccioli, Carlo Calfapietra (2018) Differences between a deciduous and a conifer tree species in gaseous and particulate emissions from biomass burning, Environmental Pollution, 2018 Mar;234:457-467. doi: 10.1016/j.envpol.2017.11.080
- Gianfranco Cardettini, Angelo Aromando, Rosa Lasaponara. Fire emission Estimation using Landsat TM: the case study studies of 2011 Fires occurred in the Ionian coast (southern Italy). 12th EARSEL Forest Fires SIG Workshop “Remote sensing of forest fire data, science and operational applications” Conference, 3-5 October 2019 - Rome, ITALY
- Hamid Reza Pourghasemi, Rosa Lasaponara. Forest fire susceptibility modelling using boosted regression tree data mining technique. 12th EARSEL Forest Fires SIG Workshop “Remote sensing of forest fire data, science and operational applications” Conference, 3-5 October 2019 - Rome, ITALY
- Karlsson C., Vajda A., Hyvärinen O.: Forest fire risk prediction on sub-seasonal and seasonal timescale in Finland, Poster presentation, EGU2019, Vienna, 7-12 April 2019
- Marco Turco, Jost von Hardenberg, Amir AghaKouchak, Maria Carmen Llasat, Antonello Provenzale & Ricardo M. Trigo (2017). On the key role of droughts in the dynamics of summer fires in Mediterranean Europe. Nature, Scientific Reports 7:81, DOI: DOI:10.1038/s41598-017-00116-9
- Marco Turco, Juan José Rosa-Cánovas, Joaquín Bedia, Sonia Jerez, Juan Pedro Montávez, Maria Carmen Llasat & Antonello Provenzale. Exacerbated fires in Mediterranean Europe due to anthropogenic warming projected with nonstationary climate-fire models (2018) Nature Communications 9:3821, DOI: 10.1038/s41467-018-06358-z
- Maria Danese, Gianfranco Cardettini, Angelo Aromando and Rosa Lasaponara. On the impacts that fire on soil and hydrogeological risk: the case study of Basilicata Region. 12th EARSEL Forest Fires SIG Workshop “Remote sensing of forest fire data, science and operational applications” Conference, 3-5 October 2019 - Rome, ITALY
- Nicola Masini, Rosa Lasaponara. Archaeology on fire. Remote sensing base approach for the damage analysis: the case of Ventarron in Peru. 12th EARSEL Forest Fires SIG Workshop “Remote sensing of forest fire data, science and operational applications” Conference, 3-5 October 2019 - Rome, ITALY

- Partanen T., Sofiev M.: A weather based prediction method to forecast regional emissions from wildfires in African grassland, Oral presentation, 12th EARSeL Fire Workshop 2019, Rome, 3-5 October 2019
- Partanen T.: A method to forecast regional emissions from wildfires in African grasslands, Oral presentation, 37th ITM Conference Hamburg, Germany, Sept. 23-27, 2019
- R. Lasaponara, M Proto CNR-IMAA, A. Aromando, G. Cardettini, V. Varela, M. Danese. On the mapping of burnt areas and burn severity using Self Organizing Map and Sentinel 2 data (in press IEEE)
- Rosa Lasaponara, Andrea Vajda, Cerdan Oliver, Vassiliki Varela, Peter Van Velthoven, Mirek Trnka, Massimiliano Pasqui, Carlo Calfapietra, Antonio Lo Porto, Brunella Rago, Emanuele Pallozzi, Nicola Afflitto, Angelo Aromando, Gianfranco Cardettini, Carmen Fattore, Monica Proto, Ari Venalainen, Cecilia Karlsson, Tero Partanen, Mikhail Sofiev, Rostislav Kouznetsov, Rosalie Vandromme, Baptiste Vignerot, Geert Jan van Oldenborgh, Folmer Krikken. Integrated services and approaches for assessing effects of climate change and extreme events for fire and post fire risk prevention. 12th EARSEL Forest Fires SIG Workshop “Remote sensing of forest fire data, science and operational applications” Conference, 3-5 October 2019 - Rome, ITALY
- Rosa Lasaponara, Angelo Aromando, Gianfranco Cardettini, Carmen Fattore, Monica Proto. Satellite based burnt areas and burn severity mapping: preliminary results in the framework of SERV-FORFIRE project. 12th EARSEL Forest Fires SIG Workshop “Remote sensing of forest fire data, science and operational applications” Conference, 3-5 October 2019 - Rome, ITALY
- Rosa Lasaponara, Angelo Aromando, Gianfranco Cardettini, Monica Proto (2018). Fire Risk Estimation at Different Scales of Observations: An Overview of Satellite Based Methods Computational Science and Its Applications – ICCSA 2018 (2018)
- Rosa Lasaponara, Biagio Tucci and Luciana Ghermandi (2018). On the Use of Satellite Sentinel 2 Data for Automatic Mapping of Burnt Areas and Burn Severity, Sustainability 2018, 10(11), 3889; https://doi.org/10.3390/su10113889
- Sofiev M., Kouznetsov R., Partanen T., Vira J., Prank M., Soares J., Tarvainen V., Vankevich R., Kukkonen J.: Finnish experience in fire smog emission estimation and pollution prediction, Oral presentation, 7th International Wildland Fire Conference Campo Grande, Brazil, 28 Oct. - 1 Nov. 2019
- Vajda A., Karlsson C., Hyvärinen O.: Sub-seasonal predictability of forest fire danger in Finland, Oral presentation, 12th EARSeL Fire Workshop 2019, Rome, 3-5 October 2019
- Vassiliki Varela, Diamando Vlachogiannis, Athanasios Sfetsos, Stelios Karozis, Rosa Lasaponara Projection of forest fire danger due to climate change in Greece. 12th EARSEL Forest Fires SIG Workshop “Remote sensing of forest fire data, science and operational applications” Conference, 3-5 October 2019 - ROME, ITALY

- Wolff C., Vajda A., Hyvärinen O.: Developing a model for forest fire risk forecast at sub-seasonal scale in Finland, FMI's Climate Bulletin: Research Letters, 1(2), 6, DOI: 10.35614/ISSN-2341-6408-IK-2019-15-RL
- Vajda A., Wolff C., Hyvärinen O., Pasqui M., Varela V., Van Velthoven P., Krikken F., Proto M., and Lasaponara R., 2020: Climate services for drought and fire danger estimation on various time scales, FMI's Climate Bulletin: Research Letters, 2(1), 14–16, DOI: https://doi.org/10.35614/ISSN-2341-6408-IK-2020-06-RL
- Meetings with the Regional State Administrative Northern Finland Agency and Rescue Services, presenting the prototype developed in the ERA4CS SERV_FORFIRE project.
- De Luca G., Modica G., Fattore C., Lasaponara R.: Unsupervised burned area mapping in a protected natural site. An approach using SAR Sentinel-1 data and k-mean algorithm. ICCSA 2020, Cagliari.
- Fattore C., De Luca G., Modica G., Lasaponara R.: On the integration of Sentinel-1 and Sentinel-2 for Mapping Burnt areas in Mediterranean heterogeneous low vegetated areas. (submitted IEEE)

4. Divulgation

NSE- New Space Economy Expoforum – Rome, 9-12 December 2019

The project was shown as poster together with the other European projects carried out by CNR-IMAA at the NSE, held in Rome on 9-12 December 2019. The first edition of NSE – New Space Economy European ExpoForum included 140 exhibitors including enterprises, research centers, institutions and startups, 184 speakers among the most influential world experts in the space sector, 60 vertical sessions on data analytics, future markets, new mobility, new space economy, new finances and new services.

EARSeL Workshop "Remote sensing of forest fire: Data, science and operational applications" – Rome, 3-5 October 2019

Sala Marconi, CNR, Piazzale Aldo Moro 7, 00185 Roma, Italy

The workshop, organized by the European Association of Remote Sensing Laboratories "EARSEL" was held in Rome at CNR headquarter from 3 to 5 October 2019. It was the 12th EARSeL Forest Fires SIG Workshop. It was chaired by Rosa Lasaponara (CNR-IMAA), Lead Principal Investigator of SERV_FORFIRE project and by Ioannis Gitas, Aristotle University of Thessaloniki, and has benefited from the presence of all the principal investigators of the project and other well-known experts, who are part of the Workshop's Scientific Committee.

Figure 49 - EARSeL Workshop "Remote sensing of forest fire: Data, science and operational applications" – Rome, 3-5 October 2019

The Workshop topic was the "Remote sensing of fire: Data, science and operational applications". The workshop has brought together experts in remote sensing, forest managers, researchers, local governments and global organizations to address the key strategic issues of fire data science, modelling, management, and monitoring. Among the invited speakers, it is worth noted, Emilio Chuvieco, Professor of Geography and director of the Environmental Ethics chair at the University of Alcalá (ES), Antonello Provenzale, Director of the Institute of Geosciences and Earth Resources, CNR (IT) and Jesus S. Miguel, Senior researcher at the European Commission Joint Research Centre.

The thematic session has included presentations and poster on the use of historical archives and data delivered by the most recent satellite missions, employing big data and time-series for:

- Dynamic modelling fire occurrence, fuel structure and fuel moisture models
- Application of image processing techniques and machine learning to support fire management
- Integration of satellite, airborne, and field sensor for wildfire management
- Fire detection and monitoring on multiple scales
- Fire behaviour and fire impacts
- Burned area, severity estimation and ecological impacts,
- Fuel consumption and fuel load estimation
- Laboratory and field studies of fire and post-fire residues
- Fire emissions estimation and air quality monitoring
- wildfire impacts and post-fire treatments.
- Exploitation of Big Earth Data and satellite time-series for fire disturbance monitoring
- Studies on the impact of climate change on forest fires occurrence and severity;
- Contribution of Sentinel missions on forest fire research;
- Improved methods of modelling post-fire vegetation trends;
- Modelling and Monitoring post fire vegetation recovery

SERV_FORFIRE project was presented by the contribution "INTEGRATED SERVICES AND APPROACHES FOR ASSESSING EFFECTS OF CLIMATE CHANGE AND EXTREME EVENTS FOR FIRE AND POST FIRE RISK PREVENTION", with the participation of all partner.

Conference website: https://cnrfire2019.eu/#organizers

Training on forest fire organized by ESA, EARSEL CNR | ESA ESRIN Frascati 30 Sep-1 Oct 2019
Training Room 9007 (Building 9), ESA ESRIN, Largo Galileo Galilei, 1, 00044 Frascati RM, Italy

On the occasion of the 12th EARSeL Forest Fires SIG Workshop, a training course was organized on the application of active and passive remote sensing techniques for fire research. The training course was held from 30 September to 1 October in Rome at European Space Agency building. The course was focused on the use of active and passive Earth Observation (EO) Technologies for fire monitoring.
EO has long been considered as a key tool for fire data, science, modelling, management, and monitoring. The most recent developments in computer technology, data processing, artificial intelligence (AI), deep learning approaches, and geospatial data mining techniques, enable advanced dynamic modelling, tools, data integration, and assimilation schemes, and are expected to significantly support and improve fire science and operational applications. Recently, the availability of new sensors from satellite, aerial, drone, and ground, along with the free access to large archives of data, has opened new perspectives for both fire science and applications.
The training was addressed to early career researchers, students, PhD students and young professionals from European institutions and Canada with background in Remote Sensing and working in topics related to wildfire. 26 Applicants from other countries have participated. The official language of the training course was English.

Figure 50 - Training on forest fire organized by ESA, EARSEL CNR | ESA ESRIN Frascati 30 Sep-1 Oct 2019

Training course website: https://cnrfire2019.eu/#training

Presentation of SERV_FORFIRE at the European Researchers' Night – Matera (Italy), 27 September 2019

The project SERV_FORFIRE was shown at the European Researchers' Night, held in Matera (Italy) on 27 September 2019, within the BRAINCITIES project, which was acknowledged as Associated Event to the European Researchers' Night. The project was shown both as a video and a panel at the European Corner, set up in the square of the University of Basilicata, where the core of the activities of the project have been realized.

Figure 51 – SERV_FORFIRE at the European Researchers' Night, Matera (Italy), 27 September 2019